CANCER GENOMICS & PROTEOMICS *18*: 735-755 (2021)
doi:10.21873/cgp.20294

Effects of Wild Yam Root *(Dioscorea villosa)* Extract on the Gene Expression Profile of Triple-negative Breast Cancer Cells

ELIZABETH MAZZIO, ABDULAZIZ ALMALKI, SELINA F. DARLING-REED and KARAM F.A. SOLIMAN

College of Pharmacy and Pharmaceutical Sciences, Institute of Public Health, Florida A&M University, Tallahassee, FL, U.S.A.

Abstract. *Background/Aim: Wild yam extract [Dioscorea villosa, (WYE)] is consistently lethal at low IC_{50}s across diverse cancer-lines in vitro. Unlike traditional anti-cancer botanicals, WYE contains detergent saponins which reduce oil-water interfacial tensions causing disintegration of lipid membranes and causing cell lysis, creating an interfering variable. Here, we evaluate WYE at sub-lethal concentrations in MDA-MB-231 triple-negative breast cancer (TNBC) cells. Materials and Methods: Quantification of saponins, membrane potential, lytic death and sub-lethal WYE changes in whole transcriptomic (WT) mRNA, miRNAs and biological parameters were evaluated. Results: WYE caused 346 differentially expressed genes (DEGs) out of 48,226 transcripts tested; where up-regulated DEGS reflect immune stimulation, TNF signaling, COX2, cytokine release and cholesterol/steroid biosynthesis. Down-regulated DEGs reflect losses in cell division cycle (CDC), cyclins (CCN), cyclin-dependent kinases (CDKs), centromere proteins (CENP), kinesin family members (KIFs) and polo-like kinases (PLKs), which were in alignment with biological studies. Conclusion: Sub-lethal concentrations of WYE appear to evoke pro-inflammatory, steroid biosynthetic and cytostatic effects in TNBC cells.*

Correspondence to: Karam F.A. Soliman Florida A & M University, College of Pharmacy and Pharmaceutical Sciences. Institute of Public Health, Room G 134 H New Pharmacy Building, 1415 ML King Blvd Tallahassee, FL 32307, U.S.A. Tel: +1 8505993306, e-mail: karam.soliman@famu.edu and Selina Darling-Reed, Florida A & M University, College of Pharmacy and Pharmaceutical Sciences, Institute of Public Health, Room G 134 H New Pharmacy Building, 1415 ML King Blvd Tallahassee, FL 32307, U.S.A. Tel: +1 8505993306, e-mail: selina.darling@famu.edu

Key Words: Immune stimulation, wild yam, *Dioscorea*, breast cancer, cell cycle.

Dioscorea villosa is a North American native plant within the genus *Dioscorea*, and the roots and rhizomes of this species are known as wild yam (1). This plant has been widely used as a botanical dietary supplement to treat menopause-related hot flashes, muscular cramps, arthritis, upset stomach, coughs, problems related to childbirth, and in cosmetic topical ointments (1). Research on the medicinal value of wild yam root extract (WYE) has shown evidence suggesting anticancer properties in particular for breast cancer and in both hormone receptor-positive and triple-negative breast cancers (TNBC), where it alters epigenetic 5-hydroxymethylcytosine DNA patterns, induces toxicity, halts cell cycle, inhibits fatty acid synthase and modifies the activity of estrogen and progesterone hormone receptors (1-5). Because TNBC is characterized by the lack of estrogen, progesterone, and human epidermal growth factor receptor 2 receptors, treatment options are limited, leading to highly aggressive metastatic cancers, with poor clinical outcomes in terms of treatment relapse and life expectancy. For this reason, a good deal of research has been focused on finding effective alternative treatments for TNBC, such as the case for WYE, which contains hundreds of constituent saponins such as deltonins, dioscoreavillosides, diarylheptanoids (6), diosgenin, and dioscin, the latter two alone can slow breast tumor growth, migration, deter stem cell phenotype and cause cell death in various models (7-11).

There is a unique element of saponin-rich plants, which vastly differs from most naturally derived plant-based chemotherapies like taxol (Taxus brevifolia), having inherent emulsification properties and a capacity to destroy fats on contact, including those housed within biological membranes (12, 13). The "on-contact" cell lytic nature of saponins was first observed in red blood cells (RBCs) in the 1920s, likened to taurocholic acid (12), which disrupts cholesterol or phosphatidylcholine rich triglycerides causing pore formation, micellular structures, lytic permeability, and cell death (13). Steroidal saponins in WYE, such as dioscin and diosgenin target phosphatidylcholine-rich membranes while triterpene saponins tend to destroy cholesterol-rich membranes (14-18);

the former can induce membrane lytic destruction within minutes (19-21).

Given that WYE and those of the *Dioscorea* species, to our knowledge, are of the most consistently cytotoxic herbs *in vitro* across diverse cancer cell lines by saponification/lytic membrane-mediated lysis (22, 23), the question remains as to effects that are occurring at concentrations (sub-lethal) that precede saponin induced lytic membrane destruction. In this work, we evaluate whole transcriptomic patterns induced by WYE at sub-lethal concentrations in MDA-MB-231 triple-negative breast cancer (TNBC) cells, where both immune stimulation and cell-cycle ablation are confirmed.

Materials and Methods

Wild yam extract (WYE) preparation. Wild Yam powder was purchased from Mountain Rose Herbs (Eugene, OR, USA). A crude WYE was prepared by dissolving the powder in absolute ethanol at 50 mg/ml, followed by vortexing and storage in the dark at –20˚C. Serial dilutions of WYE were prepared in sterile HBSS.

Cell culture. MDA-MB-231 HTB-26™ cells were purchased from ATCC. The cells were cultured in 75 cm^2 flasks with high glucose [4,500 g/l] DMEM supplemented with 7% FBS and 100 U/ml penicillin G sodium/100 μg/ml streptomycin sulfate. Cells were grown at 37˚C in 95% atmosphere 5% CO_2 and sub-cultured every three to five days. Experimental studies involving monolayers were conducted in growth media (as described above) in 96 well plates or 75 cm^2 flasks. Experimental cultures involving 3D spheroids were seeded in culture media, using low-adhesion spheroid forming 96 well plates, and pelleted by centrifugation at 1,800 × *g* for 3 min, daily for the first three days. The spheroids were grown at 37˚C in 95% atmosphere 5% CO_2 for 7 days prior to experimental treatment. Changes in morphology and live-cell imaging with FDA were captured using an inverted fluorescence microscope.

Human cytokine antibody array. Human cytokine antibody arrays (Cat# AAM-CYT-1000) (Raybiotech Inc, Peachtree Corners, GA, USA) were used to profile supernatant cytokine content. Briefly, antibody-coated array membranes were first incubated for 30 min with 1 ml of blocking buffer. After 30 min, the blocking buffer was decanted and replaced with 1 ml supernatant. Supernatants were pre-diluted in sample buffer to 20% to detect signals in highly expressed control proteins. Membranes were allowed to incubate for 5 h with shaking. Membranes were then washed with the prepared washing buffer and then incubated with 1 ml biotin-conjugated antibodies. After incubation, the mixture of biotin-conjugated antibodies was removed, and membranes were incubated with HRP-conjugated streptavidin (2 h). Detection of chemiluminescent spots was captured on Quantity One software installed on a Bio-Rad Versadoc (Bio-rad, Hercules, CA, USA), followed by densitometry analysis using NIH Image J software, microarray analysis plug-in (24). Data was imported into Raybio software data analysis sheets for final analysis.

Membrane potential and live-cell imaging. Fluorescent live cell imaging was carried out using fluorescein diacetate (FDA), which detects both plasma membrane integrity and the presence of viable cells, which retain the esterase cleaved fluorescein product (25). Tetramethyl rhodamine, ethyl ester (TMRE), was used as a permeable fluorescent cation potentiometric dye that can determine mitochondrial membrane potential in live cells (26). The loss of membrane potential and cell viability with elevated levels of saponins were captured by fluorescent imaging using an inverted fluorescent microscope.

Cell viability and proliferation. For basic toxicity experiments, cells were equally plated in 96 well plates at 0.5×10^6 cells/ml. Resazurin (Alamar Blue) indicator dye was used to measure cell viability as an indicator of basic metabolic rate (27). Briefly, a working solution of resazurin (0.5 mg/ml) was prepared in sterile PBS; filter sterilized through a 0.2-micron filter, added to the samples [15% (v/v) equivalent], and returned to the incubator for 2-6 h. Reduction of the dye by viable cells reduced the oxidized resazurin, yielding a bright red fluorescent intermediate resorufin quantified using a Synergy HTX multi-mode reader (Bio-Tek, Winooski, VT, USA) using the following settings: 530 nm (excitation)/590 nm (emission) filters. Cell proliferation assays were conducted over 6 days, where cells were equally plated in 96 well plates at 0.05×10^6 cells/ml in culture media in the absence or presence of a varying concentration of WYE.

Saponin foam test. In this study, the stable foaming properties of the saponins in WYE were tested and correlated to the cytotoxic effects of the yam extract. In brief, 500 mg of wild yam root (powdered) was added to 10 ml of sterile water (50 mg/ml) and boiled for 5 min, followed by filtration through a 0.4-micron mesh filter. Serial dilutions of the filtrate were prepared in sterile water (room temperature) in separate glass test tubes, which were stopped and shaken vigorously for about 30 seconds. Samples were allowed to stand for one-half h. Honeycomb froth indicated saponins, where images were captured, and the foam area quantified using Image J analysis software (20).

Microarray WT 2.1 human datasets. All cells were washed three times in ice-cold HBSS, rapidly frozen, and stored at –80˚C. Total RNA was isolated and purified using the Trizol/chloroform method. The quality was assessed, and concentration was equalized to 82 ng/μl in nuclease-free water. Whole transcriptome analysis was conducted according to the GeneChip TM WT PLUS Reagent Manual for Whole Transcript (WT).

Expression arrays. Briefly, RNA was synthesized to the first-strand cDNA, then second-strand cDNA, followed by a subsequent transcription to cRNA. cRNA was purified and assessed for yield prior to 2nd cycle single-stranded cDNA synthesis, hydrolysis of RNA, and purification of 2nd cycle single-stranded cDNA. cDNA was then quantified for yield and equalized to 176 ng/ml. Subsequently, cDNA was fragmented, labeled, and hybridized onto the arrays prior to being subjected to fluidics and imaging using the Gene Atlas (Affymetrix, ThermoFisher Scientific). The array data quality control and initial processing from CEL to CHP files were conducted using an expression console, prior to data evaluation using the Affymetrix transcriptome analysis console, String Database (String Consortium 2020) and DAVID functional annotation microarray tools (28-30), n=3. The dataset has been deposited to NIH Gene Expression Omnibus located at: https://www.ncbi.nlm.nih.gov/geo/query/acc.cgi?acc=GSE180621.

ELISA for IL-8. Supernatants from MDA-MB-231 cells (Control *vs*. WYE Lo 15 μg/ml) were collected and centrifuged at 1,000 × *g* for 5 min at 4˚C. Specific ELISA was performed using IL-8 ELISA kit

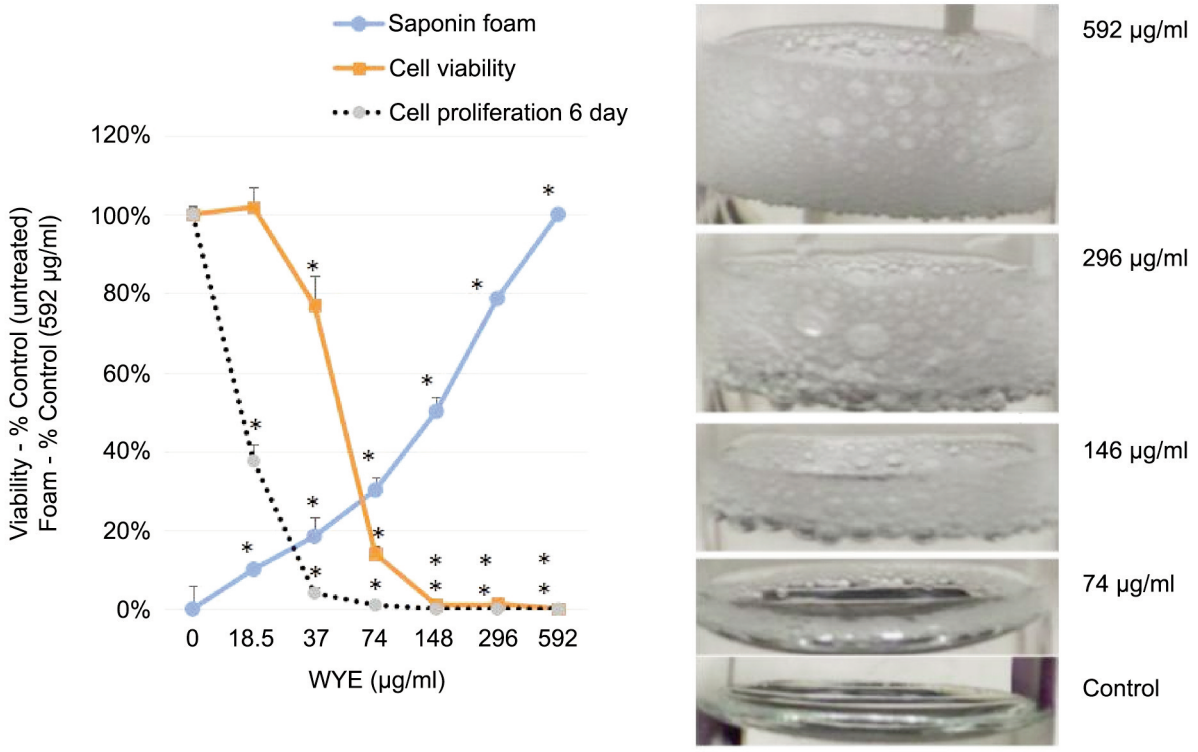

Figure 1. *Cytotoxic and cytostatic effects related to saponin content of WYE in MDA-MB-231 cells. The data represent the mean±S.E.M, n=4 for cell viability (at 24 h), cell proliferation (at 6 days) plotted as % (untreated) controls and WYE saponin foam (where 592 µg/ml was set at 100% control), n=3. Significant differences between the controls and treatment groups were determined by a one way ANOVA, followed by a Tukey post hoc test ,*p<0.05. The gene chip icons, represent the 2 concentrations at which microarray analysis work was conducted representing WYE sub-lethal Low (15 µg/ml) and WYE sub-lethal High (30 µg/ml).*

following manufacturer's instructions (Human IL-8/CXCL8 ELISA) (Millipore-Sigma, Saint Louis, MO, USA). The sample was diluted in buffer 20% supernatant/buffer, and 100 µl of prepared supernatant from samples was added to 96 well plates pre-coated with the capture antibody. After incubation, 100 µl of prepared biotinylated antibody mixture was added to each well. After 1 h, the mixture was decanted, and 100 µl streptavidin solution was placed in each well and incubated. Substrate reagent (100 µl) was then added to each well for 30 min followed by a 50 µl stop solution. Plates were read at 450 nm using a Biotek H.T.X. Synergy-multi-mode microplate reader.

Statistical analysis. Statistical analysis was performed for the basic studies using GraphPad Prism (version 3.0; Graph Pad Software Inc., San Diego, CA, USA). The significance of the difference between the groups was assessed using either a student's *t*-test or a one-way ANOVA followed by Tukey *post hoc* analysis.

Results

Both cytostatic and cytotoxic curves were generated over a dose-response of WYE, where saponins were quantified by a simple foam test (Figure 1). The data show a close correlation between foam and cell death, with the (anti-proliferative) cytostatic effects being in close proximity to/but slightly preceding sub-lethal concentrations of WYE. At this point, it is uncertain whether the loss of the cell cycle is related to basic cytotoxicity given the proximity of these curves, which will be further elucidated in this work. Next, the data show that greater saponin content in higher concentrations of WYE are associated with cell death, which coincides closely to damage to lipid membrane bio-layers. In Figure 2, we show basic fluorescent cell imaging of plasma membrane integrity/viability (left panel) and mitochondrial membrane (right) using fluorescent probes FDA and TMRE, respectively. The data show complete loss of both with greater saponin foam content in WYE. To determine if WYE saponins would also destroy a small 3D tumor spheroid, we evaluated cell survival (FDA) and morphological changes with increasing concentration of WYE (Figure 3). The data show spheroid tumors to be slightly more resistant to WYE, however, at concentrations exceeding 148 µg/ml there was near complete death of the entire spheroid.

For microarray studies, we chose to conduct experimentation at 2 sub-lethal concentrations denoted as Low (15 µg/ml); sub-lethal and High (30 µg/ml); sub-lethal/cusp of death (Figure 4).

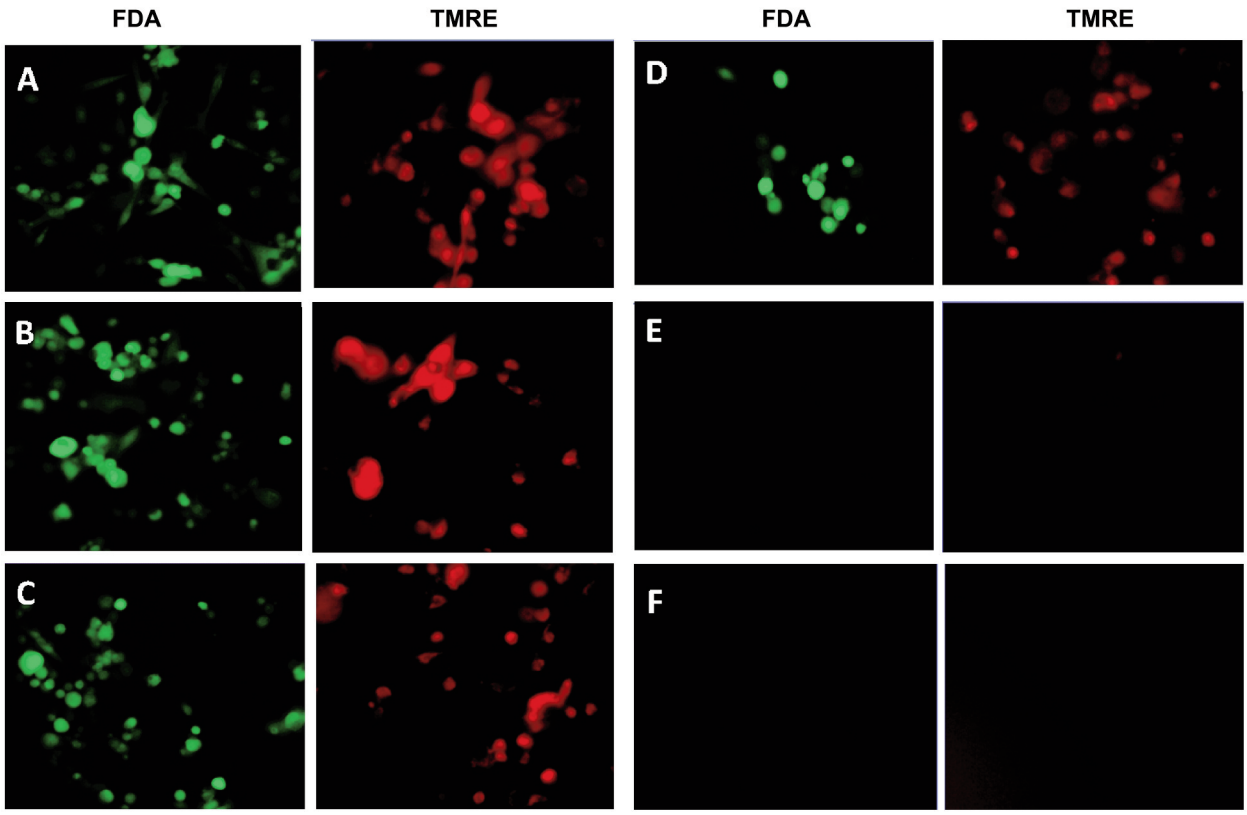

Figure 2. *Effect of WYE on cell membrane potentials (plasma/viability) obtained with FDA (left panel) and mitochondrial TMRE (right panel). (A) Control, WYE Treatment (B) 18.5 μg/ml, (C)37 μg/ml, (D) 74 μg/ml, (E) 148 μg/ml, (F) 296 μg/ml).*

Cells for microarray studies were prepared in 75 cm2 flasks and monitored to ensure no morphological structure or attachment changes occurred over 24 h of treatment prior to cell pellet collection. Both cell pellets and supernatant were collected from the same samples and stored at –80˚C. While we provide whole transcriptomic data on both sets, we focus the analysis within this article on only the WYE (low *vs.* control) data set. In both sets, less than 0.7% of the whole transcriptome showed differentially expressed genes (DEGs), with criteria set at -2<x>+2-fold change, *p*-Value, and FDR *p*-Values <0.05. The data for DEGs in the WYE sub-lethal (low) *vs.* control groups are presented in Table I, with both sets, including sub-lethal WYE (high) *vs.* control provided at https://www.ncbi.nlm.nih.gov/geo/query/acc.cgi?acc=GSE180621.

Using Stringdb, all down-regulated genes meeting criteria for WYE (low) were entered, and relational networks were identified (Figure 5). The data show a statistical loss in gene elements that transcribe for cell cycle and mitosis, showing a network FDR value for biological processes analysis (gene ontology) *p*-Value <0.235e-83. High significance for changes in the chromosome, cell division, DNA replication, and cross strand repair using local network cluster (STRING) also show FDR *p*-values up to p<4.48e-63. All database platforms pickup up this differential as significant, including the Reactome and Kyoto Encyclopedia of Genes and Genomes (Kegg) pathways, where the latter was also found in the WIKIpathway report of Affymetrix/applied Biosystems transcriptome analysis console report (including up and down DEGs) (Figure 6). Similarly, stringdb analysis was performed on up-regulated DEGs for WYE (Low) (Figure 7), where most significant changes centered on steroid synthesis and cytokine signaling, specifically affecting the TNF-alpha pathway, changes also reflected in the component Kegg overlap map (Figure 8).

The supernatant of the samples matching the microarray was tested for the presence of cytokines using antibody arrays where the largest up-regulated differential DEG by WYE was for CXCL8/ IL-8, being observed in densitometry values within the anti-body array itself (Figure 9A,B), the Affymetrix microarray (Figure 10) and confirmed by Elisa (Figure 11). Figure 9A,B shows the relative comparison of cytokines released in the supernatant and the mRNA in cells, where the criteria for gene analysis was lowered to less than 2-fold, with a significant *p*-Value <0.05 and no filter on FDR

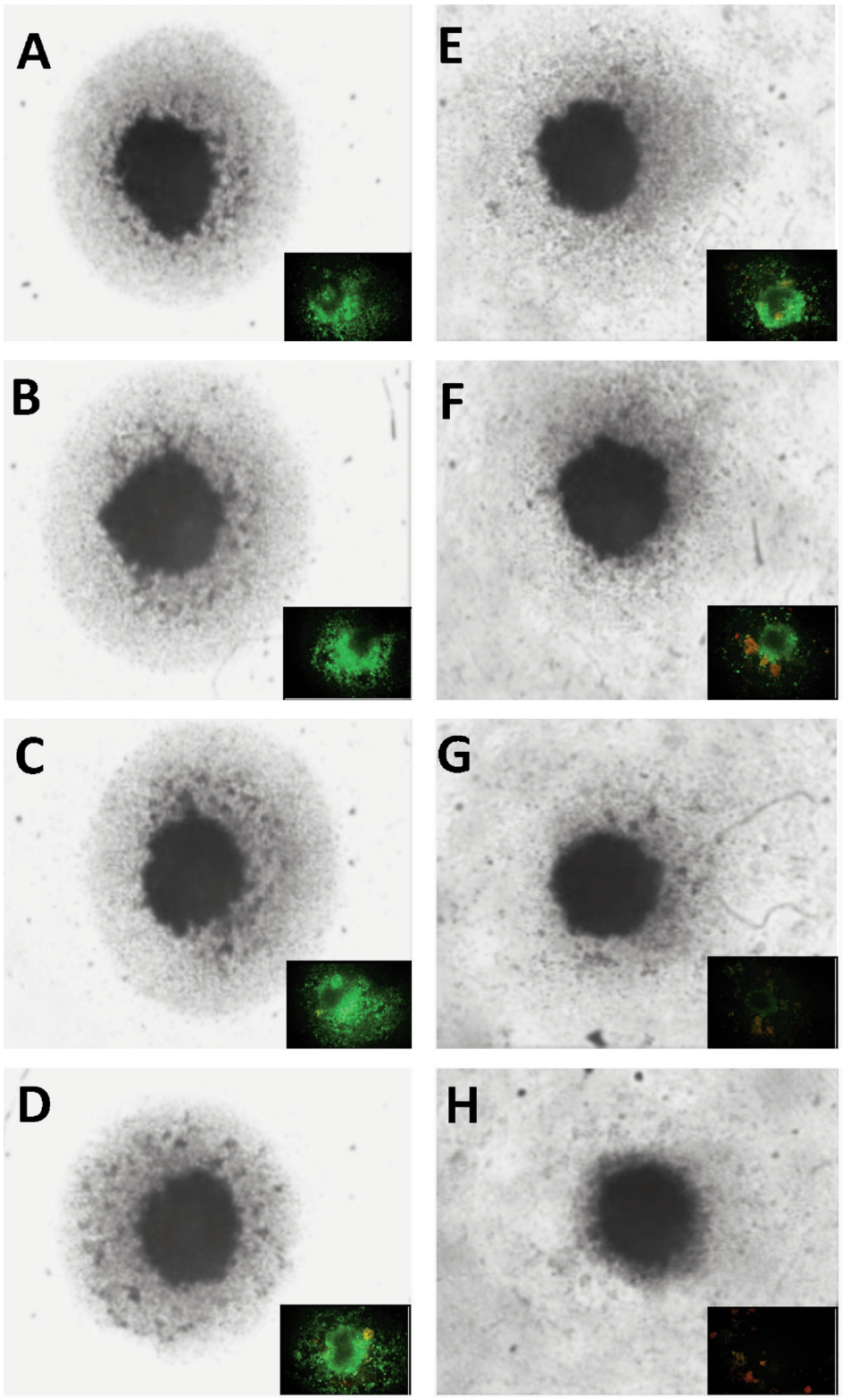

Figure 3. *Effect of WYE on 3D tumor spheroids. Cell viability and morphological changes in MDA-MB-231 tumor spheroids with increasing concentration of WYE are shown. The data represent basic changes in spheroid structure (main image; black and white), with fluorescent FDA viable cell staining (green) in the lower left section of each main image. (A) Control, WYE Treatment (B) 4.62 μg/ml, (C) 9.25 μg/ml, (D) 18.5 μg/ml, (E) 37 μg/ml, (F) 74 μg/ml, (G) 148 μg/ml, (H) 296 μg/ml.*

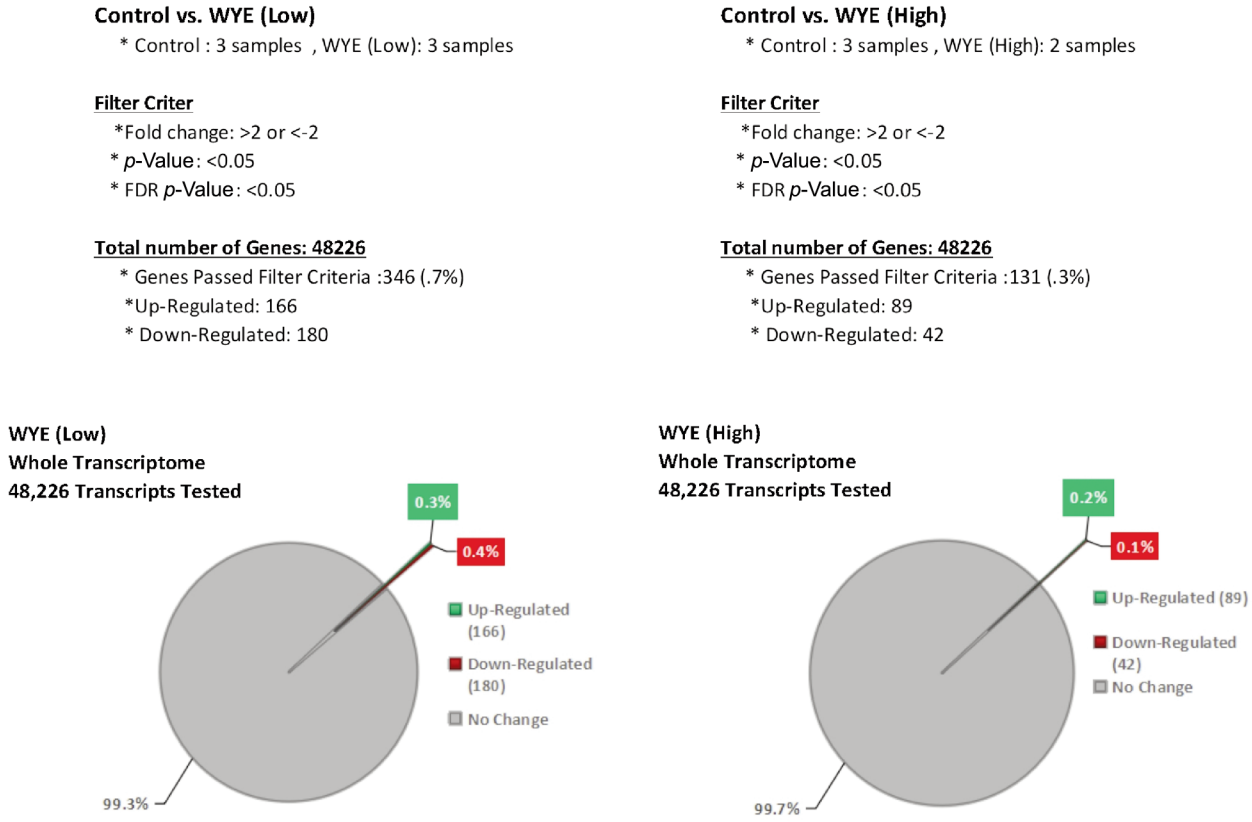

Figure 4. *Microarray gene summary report. Overview of DEGs expressed when comparing controls (untreated) n=3 vs. WYE (Low, sub-lethal at 15 ug/ml) n=3 or WYE (High, sub-lethal cusp of cell death at 30 ug/ml). The data selection criteria were set at -2<x>+2 fold change, p-Value <0.05 and FDR p-Value <0.05.*

p-Values. There was a high degree of matching values between proteins released in the supernatant and the mRNA transcription for those proteins in the same pellet sample. In summary, this provides an overall snapshot of the effects of WYE in MDA-MB-231 cells at sub-lethal concentrations.

Discussion

In this study, we evaluate the biological and transcriptomic effects of WYE on TNBC cells at sub-lethal concentrations, well below the point involving saponin-mediated cell lysis. WYE shows antiproliferative effects at sub-lethal concentration tantamount to severe downregulation of gene transcripts involved in mitosis and cell division, including transcripts of the following classes: cell division cycle (CDC), cysteine-rich protein 61, connective tissue growth factor, and nephroblastoma overexpressed (CCN), cyclin-dependent kinases (CDK), centromere proteins (CENPs), kinesin superfamily transcripts (KIFS), and polo-like kinases (PLK). These effects were concurrent with single gene up-regulation of the p21 gene CDKN1A, all of which are likely responsible for the observed cytostatic effects of WYE in a 6-day proliferation study. Our findings in this aspect support much of the existing literature for WYE and saponins from the *Dioscorea* species having the capacity to induce cell-cycle arrest (G_2/M) across diverse cancer cell lines with observed downregulation of a similar list of cyclins and cell cycle regulatory transcripts (Cdc25C, Cdk1) (31-34).

While WYE was able to halt cell division effectively at low concentrations (15 μg/ml), the data in this work show an apparent rise in a series of genes that demarcate immune stimulation. As to the compounds responsible for these effects, they could be one or more of the known hundreds of compounds present in the root, such as diterpenes, phenolics, cyanidins, quinones, methyl parvifloside, trigofoenoside A-1, protodeltonin, deltonin, glucosidodeltonin, zingiberensis I, methylprotodioscin, zingiberensis, dioscin, prosapogenin, dioscoreavillosides A and B, diarylheptanoids or possibly lipidated steroid saponins (6).

Table I. *Effects of WYE on the transcriptome in MDA-MB-231 cells. Selection criteria include greater than or less than 2 fold change and both p-Values and FDR p-values <0.05. The data is presented as the effects of WYE on transcript by Fold Change, Gene Symbol, Gene Description, and significance.*

Transcriptome changes: Control *vs*. WYE (Low 15 μg/ml).

Gene symbol	Description	Fold change	*p*-Value	FDR *p*-Value
CXCL8	Chemokine (C-X-C motif) ligand 8	9.09	3.79E-10	1.83E-05
KLF2	Kruppel-like factor 2	7.82	4.67E-07	1.90E-03
RHOB	Ras homolog fam. mem. B	7.64	1.08E-09	2.60E-05
IL1A	Interleukin 1 alpha	7.53	1.15E-05	6.50E-03
PTGS2	Prostaglandin-endoperoxide synthase 2 [COX-2]	7.01	1.59E-06	2.80E-03
HMOX1	Heme oxygenase 1	5.79	1.75E-06	2.80E-03
NR1D1	Nuclear receptor subfam. 1, group D, mem. 1	5.45	5.65E-07	2.10E-03
HKDC1	Hexokinase d.c. 1	5.36	5.50E-05	1.29E-02
GEM	GTP b.p overexpressed in skeletal muscle	5.29	1.46E-07	7.00E-04
HMGCS1	3-hydroxy-3-methylglutaryl-CoA synthase 1 (soluble)	5.28	9.36E-08	5.00E-04
INSIG1	Insulin induced gene 1	5.25	2.24E-08	3.00E-04
ATF3	Activating transcription factor 3	4.94	4.95E-06	5.00E-03
DUSP10	Dual specificity phosphatase 10	4.91	6.61E-06	5.70E-03
GDF15	Growth differentiation factor 15	4.90	6.16E-07	2.10E-03
KDM7A	Lysine (K)-specific demethylase 7A	4.88	8.70E-08	5.00E-04
EGR1	Early growth response 1	4.74	1.99E-05	8.00E-03
TNFAIP3	Tumor necrosis factor, alpha-induced protein 3	4.65	6.86E-07	2.10E-03
LOC105378662	Uncharacterized LOC105378662; LOC105378663	4.32	7.74E-06	5.70E-03
TM4SF19	TM4SF19; TCTEX1D2; TM4SF19-TCTEX1D2	4.26	2.18E-06	3.00E-03
RRAD	Ras-related associated with diabetes	4.21	5.85E-08	5.00E-04
STC1	Stanniocalcin 1	4.09	7.30E-08	5.00E-04
FBXO32	F-box protein 32	3.86	1.00E-04	1.80E-02
KLHL24	Kelch-like fam. mem. 24	3.85	1.62E-06	2.80E-03
BACH1-IT2	BACH1 intronic transcript 2	3.75	1.64E-05	7.50E-03
CREBRF	CREB3 regulatory factor	3.71	1.87E-05	7.90E-03
ZFPM2-AS1	ZFPM2 antisense RNA 1	3.69	1.71E-05	7.50E-03
ABTB2	Ankyrin repeat and BTB (POZ) d.c. 2	3.64	2.89E-05	9.70E-03
LOC105373713	Uncharacterized LOC105373713	3.55	6.22E-05	1.33E-02
YPEL2	Yippee like 2	3.53	7.57E-07	2.10E-03
EID3	EP300 interacting inhibitor of differentiation 3	3.48	3.00E-04	3.26E-02
CDKN1A	Cyclin-dependent kinase inhibitor 1A (p21, Cip1)	3.46	6.19E-05	1.33E-02
ZNF114	Zinc finger protein 114	3.40	9.59E-06	6.00E-03
PLEKHM1	Pleckstrin homology, fam. M (w.RUN domain) mem. 1	3.37	6.46E-06	5.70E-03
SLC2A3	Solute carrier fam. 2 (facilitated glucose), m 3	3.37	8.34E-07	2.20E-03
KLF7	Kruppel-like factor 7 (ubiquitous)	3.34	1.00E-04	1.73E-02
IL11	Interleukin 11	3.33	3.00E-04	3.09E-02
KPNA7	Karyopherin alpha 7 (importin alpha 8)	3.24	9.69E-06	6.00E-03
SIK1	Salt-inducible kinase 1	3.22	3.00E-04	3.18E-02
ZBTB10	Zinc finger and BTB d.c. 10	3.21	4.00E-04	3.96E-02
IRAK2	Interleukin 1 receptor associated kinase 2	3.19	2.00E-04	2.15E-02
KLF9	Kruppel-like factor 9	3.18	8.04E-06	5.90E-03
RASGEF1B	RasGEF domain fam. mem. 1B	3.14	4.89E-06	5.00E-03
TMEM159	Transmembrane protein 159	3.11	9.17E-06	6.00E-03
HIST1H2BD	Histone cluster 1, H2bd	3.10	4.00E-04	3.83E-02
MIR4315-1	MicroRNA 4315-1;2 PLEKHM1	3.09	1.06E-05	6.30E-03
CBLB	Cbl proto-oncogene B, E3 ubiquitin protein ligase	3.05	1.60E-05	7.50E-03
ICAM1	Intercellular adhesion molecule 1	3.05	3.00E-04	2.87E-02
GFPT2	Glutamine-fructose-6-phosphate transaminase 2	3.03	9.73E-06	6.00E-03
UAP1L1	UDP-N-acetylglucosamine pyrophosphorylase 1 like 1	3.03	2.00E-04	2.15E-02
NPC1	Niemann-Pick disease, type C1	3.01	1.90E-05	7.90E-03
GAB2	GRB2-associated b.p 2	2.98	1.20E-05	6.70E-03
JUNB	Jun B proto-oncogene	2.98	6.79E-05	1.39E-02
DSC2	Desmocollin 2	2.97	8.50E-06	5.90E-03
MXD1	MAX dimerization protein 1	2.96	5.60E-06	5.20E-03

Table I. *Continued*

Table I. *Continued*

Gene symbol	Description	Fold change	*p*-Value	FDR *p*-Value
GABARAPL1	GABA(A) receptor-associated protein like 1	2.95	1.39E-05	7.20E-03
FRZB	Frizzled-related protein	2.93	1.38E-06	2.80E-03
TP53INP1	Tumor protein p53 inducible nuclear protein 1	2.91	3.34E-07	1.50E-03
RRAGC	Ras-related GTP binding C	2.89	2.07E-06	3.00E-03
GRB10	Growth factor receptor bound protein 10	2.87	1.74E-05	7.60E-03
KDM6B	Lysine (K)-specific demethylase 6B	2.87	1.00E-04	1.90E-02
JUND	Jun D proto-oncogene	2.84	2.87E-05	9.70E-03
LSS	Lanosterol synthase	2.84	2.00E-04	2.19E-02
TCP11L2	T-complex 11, testis-specific-like 2	2.82	1.75E-06	2.80E-03
HBP1	HMG-box transcription factor 1	2.80	6.98E-05	1.40E-02
ABL2	ABL proto-oncogene 2, non-receptor tyrosine kinase	2.75	2.28E-05	8.50E-03
FLCN; PLD6	Golliculin; phospholipase D fam., mem. 6	2.75	4.37E-05	1.17E-02
BACH1	BTB and CNC homology 1, BLZTF 1	2.73	6.29E-05	1.33E-02
KLF6	Kruppel-like factor 6	2.73	2.10E-05	8.10E-03
DENND2C	DENN/MADD d.c. 2C	2.72	6.70E-06	5.70E-03
TRAF1	TNF receptor-associated factor 1	2.71	1.00E-04	2.03E-02
MSMO1	Methylsterol monooxygenase 1	2.70	1.56E-06	2.80E-03
PGM2L1	Phosphoglucomutase 2-like 1	2.70	2.00E-04	2.68E-02
C3orf52	Chromosome 3 open reading frame 52	2.69	2.00E-04	2.23E-02
LHFPL2	Lipoma HMGIC fusion partner-like 2	2.69	7.62E-06	5.70E-03
CXCL2	Chemokine (C-X-C motif) ligand 2	2.68	2.00E-04	2.75E-02
FNIP1	Folliculin interacting protein 1	2.68	7.67E-06	5.70E-03
TLR8-AS1	TLR8 antisense RNA 1	2.67	1.00E-04	1.86E-02
PLIN2	Perilipin 2	2.61	5.37E-06	5.10E-03
SMOX	Spermine oxidase	2.61	4.00E-04	3.36E-02
ZFYVE1	Zinc finger, FYVE d.c. 1	2.59	6.51E-05	1.36E-02
FTH1	Ferritin, heavy polypeptide 1	2.58	7.07E-06	5.70E-03
USP53	Ubiquitin specific peptidase 53	2.58	7.49E-06	5.70E-03
TRPV3	Transient receptor potential cation channel, sub-V, mem. 3	2.57	2.00E-04	2.09E-02
SLC43A2	Solute carrier fam. 43 (amino acid), mem. 2	2.56	3.00E-04	3.35E-02
DDIT3	DNA-damage-inducible transcript 3	2.54	4.22E-06	4.60E-03
SOD2	Superoxide dismutase 2, mitochondrial	2.53	5.88E-06	5.30E-03
PIM1	Pim-1 proto-oncogene, serine/threonine kinase	2.52	2.60E-05	9.30E-03
CD83	CD83 molecule	2.51	4.00E-04	3.93E-02
HSPA1A; HSPA1B	Heat shock 70kDa protein 1A; 1B	2.50	1.85E-05	7.90E-03
CRYM-AS1	CRYM antisense RNA 1	2.49	1.38E-05	7.20E-03
DUSP8	Dual specificity phosphatase 8	2.49	7.99E-05	1.48E-02
SPDYA	Speedy/RINGO cell cycle regulator fam. mem. A	2.47	2.45E-05	8.90E-03
KIAA1551	KIAA1551	2.46	3.67E-05	1.07E-02
ERN1	Endoplasmic reticulum to nucleus signaling 1	2.45	7.36E-05	1.42E-02
NPPA-AS1	NPPA antisense RNA 1	2.45	3.12E-05	1.00E-02
PNRC1	Proline-rich nuclear receptor coactivator 1	2.44	1.00E-04	1.81E-02
LOC101929125	Uncharacterized LOC101929125	2.44	4.32E-06	4.60E-03
CSF1	Colony stimulating factor 1 (macrophage)	2.41	1.00E-04	1.86E-02
ZC3H12C	Zinc finger CCCH-type containing 12C	2.41	3.00E-04	2.95E-02
ITGB3	Integrin beta 3	2.40	4.23E-05	1.16E-02
NOV	Nephroblastoma overexpressed	2.40	2.00E-04	2.09E-02
TBC1D7	TBC1 domain fam., mem. 7	2.40	2.70E-05	9.40E-03
HMGCR	3-hydroxy-3-methylglutaryl-CoA reductase	2.39	2.66E-06	3.50E-03
IL6R	Interleukin 6 receptor	2.39	1.00E-04	1.81E-02
MMP1	Matrix metallopeptidase 1	2.38	5.01E-06	5.00E-03
HSPA1B; HSPA1A	Heat shock 70kDa protein 1B; 1A	2.37	9.02E-05	1.60E-02
JUN	Jun proto-oncogene	2.37	2.25E-05	8.50E-03
GAREM1	GRB2 associated regulator of MAPK1 1	2.34	9.89E-05	1.68E-02
MIR616; DDIT3	microRNA 616; DNA-damage-inducible transcript 3	2.33	4.72E-05	1.22E-02
PER1	period circadian clock 1	2.33	2.00E-04	2.61E-02
NEU1	Sialidase 1 (lysosomal sialidase)	2.33	7.43E-05	1.42E-02
DHRS9	dehydrogenase/reductase (SDR fam.) mem. 9	2.32	3.52E-05	1.05E-02

Table I. *Continued*

Table I. *Continued*

Gene symbol	Description	Fold change	*p*-Value	FDR *p*-Value
LRRC37B	Leucine rich repeat containing 37B	2.32	4.00E-04	3.74E-02
ATP6V0D2	ATPase, H+ tr, lysosomal 38kDa, V0 su. d2	2.31	3.49E-05	1.05E-02
FOXC1	Forkhead box C1	2.31	2.00E-04	2.49E-02
SQLE	Squalene epoxidase	2.30	5.31E-05	1.28E-02
JARID2	Jumonji, AT rich interactive domain 2	2.29	2.00E-04	2.27E-02
UGDH	UDP-glucose 6-dehydrogenase	2.29	1.25E-05	6.80E-03
LOC105379177	Uncharacterized LOC105379177	2.29	6.29E-05	1.33E-02
LDLR	Low density lipoprotein receptor	2.28	6.00E-05	1.32E-02
NFKBIA	NFK light polypeptide gene enh B-cells inhibitor, alpha	2.28	4.29E-05	1.16E-02
AHNAK2	AHNAK nucleoprotein 2	2.27	2.00E-04	2.68E-02
CEBPB	CCAAT/enhancer b.p (C/EBP), beta	2.27	8.36E-05	1.53E-02
DTNA	Dystrobrevin, alpha	2.26	5.00E-04	4.10E-02
SPAG9	Sperm associated antigen 9	2.26	2.06E-05	8.00E-03
CYTH1	Cytohesin 1	2.25	2.00E-04	2.34E-02
FAM102A	Fam. with sequence similarity 102, mem. A	2.25	1.00E-04	1.74E-02
RNF19B	Ring finger protein 19B	2.25	4.00E-04	3.72E-02
ZBTB43	Zinc finger and BTB d.c. 43	2.25	5.62E-05	1.30E-02
IDI1	Isopentenyl-diphosphate delta isomerase 1	2.24	8.46E-06	5.90E-03
CHD2	Chromodomain helicase DNA b.p 2	2.23	6.97E-05	1.40E-02
IL6	Interleukin 6	2.23	2.00E-04	2.16E-02
NDRG1	N-myc downstream regulated 1	2.23	3.94E-05	1.13E-02
BHLHE40	Basic helix-loo*p*-helix fam., mem. e40	2.22	3.29E-05	1.04E-02
IER3	Immediate early response 3	2.21	1.00E-04	1.70E-02
LIF	Leukemia inhibitory factor	2.21	1.00E-04	1.80E-02
ZNF165	Zinc finger protein 165	2.21	2.00E-04	2.14E-02
BTG1; LINC01619	B-cell translocation gene 1, LINE RNA 1619	2.20	6.00E-04	4.57E-02
PMP22	Peripheral myelin protein 22	2.19	1.65E-05	7.50E-03
THEMIS2	Thymocyte selection associated fam. mem. 2	2.19	8.30E-05	1.53E-02
CD55	CD55 molecule, decay accelerating factor	2.17	1.51E-05	7.40E-03
DUSP16	Dual specificity phosphatase 16	2.17	1.00E-04	1.70E-02
SOX4	SRY box 4	2.17	2.00E-04	2.39E-02
LOC105369949	Uncharacterized LOC105369949	2.17	4.00E-04	3.87E-02
LOC105379695	Uncharacterized LOC105379695	2.17	6.02E-05	1.32E-02
FZD8; MIR4683	Frizzled class receptor 8; MicroRNA 4683	2.16	4.00E-04	3.74E-02
CLDN4	Claudin 4	2.14	4.00E-04	3.64E-02
LINC-PINT	Long intergenic non-protein coding RNA, p53	2.13	2.00E-04	2.17E-02
IRS2	Insulin receptor substrate 2	2.12	2.00E-04	2.34E-02
MCOLN3	Mucolipin 3	2.12	5.50E-05	1.29E-02
STARD4	StAR-related lipid transfer d.c. 4	2.12	4.09E-05	1.16E-02
CTSL	Cathepsin L	2.11	1.00E-04	1.89E-02
RHOF	Ras homolog fam. mem. F (in filopodia)	2.11	6.00E-04	4.93E-02
TIPARP	TCDD-inducible poly(ADP-ribose) polymerase	2.11	2.00E-04	2.17E-02
STX3; OR10Y1P	Syntaxin 3; olfactory receptor, Fam. 10, subfam. Y, mem. 1pg	2.10	2.00E-04	2.43E-02
PELI1	Pellino E3 ubiquitin protein ligase 1	2.08	5.16E-05	1.27E-02
YOD1	YOD1 deubiquitinase	2.08	3.00E-04	3.16E-02
CYP51A1; LRRD1	Cytochrome P450, f51, subfam. A, 1; LRR and DDC 1	2.07	3.16E-05	1.00E-02
IRF9	Interferon regulatory factor 9	2.07	4.00E-04	3.43E-02
AGPAT4	1-acylglycerol-3-phosphate O-acyltransferase 4	2.05	2.34E-05	8.60E-03
HDAC9	Histone deacetylase 9	2.05	3.00E-04	2.97E-02
ZCCHC14	Zinc finger, CCHC d.c. 14	2.05	6.00E-04	4.95E-02
JMJD1C	Jumonji d.c. 1C	2.02	6.00E-04	4.96E-02
SQSTM1	Sequestosome 1	2.02	1.00E-04	1.89E-02
KLF3	Kruppel-like factor 3 (basic)	2.01	3.00E-05	9.80E-03
TFPI2	Tissue factor pathway inhibitor 2	2.01	9.34E-05	1.64E-02
AJUBA	Ajuba LIM protein	-2.00	5.00E-04	3.97E-02
KNTC1	Kinetochore associated 1	-2.00	1.00E-04	1.70E-02
POLR3B	Polymerase (RNA) III (DNA directed) polypeptide B	-2.00	2.00E-04	2.25E-02
SASS6	SAS-6 centriolar assembly protein	-2.00	1.00E-04	1.95E-02

Table I. *Continued*

Table I. *Continued*

Gene symbol	Description	Fold change	*p*-Value	FDR *p*-Value
HMGB2	High mobility group box 2	-2.01	3.00E-04	3.26E-02
BIRC5	Baculoviral IAP repeat containing 5	-2.02	7.84E-05	1.46E-02
GLMN	Glomulin, FKBP associated protein	-2.02	3.00E-04	2.94E-02
HIST1H2AJ	Histone cluster 1, H2aj	-2.02	3.00E-04	2.87E-02
ZNF738	Zinc finger protein 738	-2.02	5.76E-05	1.31E-02
CHRNA5	Cholinergic receptor, nicotinic alpha 5	-2.03	4.47E-05	1.18E-02
NCAPD3	Non-SMC condensin II complex su. D3	-2.03	7.60E-05	1.43E-02
RMI1	RecQ mediated genome instability 1	-2.03	4.00E-04	3.93E-02
CDCA7L	Cell division cycle associated 7-like	-2.04	2.00E-04	2.17E-02
FAM111A	Fam. with sequence similarity 111, mem. A	-2.04	9.96E-05	1.68E-02
FANCB	Fanconi anemia complementation group B	-2.04	2.00E-04	2.44E-02
LIN9	Lin-9 DREAM MuvB core complex component	-2.04	7.89E-05	1.47E-02
MYBL1	V-myb avian myeloblastosis viral oncogene homolog-like 1	-2.04	1.62E-05	7.50E-03
CEP192	Centrosomal protein 192kDa	-2.06	5.00E-04	4.23E-02
CCNF	Cyclin F	-2.07	3.44E-05	1.05E-02
STIL	SCL/TAL1 interrupting locus	-2.07	2.00E-04	2.27E-02
DHFR	Dihydrofolate reductase	-2.08	2.00E-04	2.34E-02
E2F8	E2F transcription factor 8	-2.08	9.40E-06	6.00E-03
RAD54B; FSBP	RAD54 homolog B; fibrinogen Silencer b.p	-2.08	2.00E-04	2.34E-02
SPRY1	Sprouty RTK signaling antagonist 1	-2.08	4.00E-04	3.62E-02
TPX2	TPX2, microtubule-associated	-2.08	5.58E-05	1.30E-02
DSN1	DSN1 homolog, MIS12 kinetochore complex component	-2.09	3.00E-04	2.87E-02
CHAC2	ChaC, cation transport regulator homolog 2 (E. coli)	-2.10	3.44E-05	1.05E-02
PLK1	Polo-like kinase 1	-2.10	4.13E-05	1.16E-02
PLK2	Polo-like kinase 2	-2.10	1.60E-05	7.50E-03
CASC5	Cancer susceptibility candidate 5	-2.11	2.00E-04	2.56E-02
CEP55	Centrosomal protein 55kDa	-2.11	1.00E-04	1.93E-02
PRIMPOL	Primase and DNA directed polymerase	-2.11	5.00E-04	4.01E-02
YEATS4	YEATS d.c. 4	-2.11	6.21E-05	1.33E-02
HSPA14	Heat shock 70kDa protein 14	-2.12	9.58E-05	1.66E-02
PRC1	Protein regulator of cytokinesis 1	-2.12	8.98E-05	1.60E-02
CENPQ	Centromere protein Q	-2.13	2.00E-04	2.49E-02
MTBP	MDM2 b.p	-2.13	2.00E-04	2.16E-02
RFC5	Replication factor C su. 5	-2.13	8.72E-05	1.56E-02
SLCO4A1	Solute carrier organic anion transporter fam., mem. 4A1	-2.13	1.00E-04	2.02E-02
SKA1	Spindle and kinetochore associated complex su. 1	-2.13	2.00E-04	2.55E-02
TICRR	TOPBP1-interacting checkpoint and replication regulator	-2.13	1.00E-04	1.70E-02
EZH2	Enhancer of zeste 2 polycomb repressive complex 2 su.	-2.14	6.16E-05	1.33E-02
RAD51	RAD51 recombinase	-2.14	2.19E-05	8.30E-03
STAMBPL1	STAM b.*p*-like 1	-2.14	4.40E-05	1.17E-02
WDHD1	WD repeat and HMG-box DNA b.p 1	-2.14	2.00E-04	2.49E-02
ZNF93	Zinc finger protein 93	-2.14	1.00E-04	1.70E-02
HAUS8	HAUS augmin like complex su. 8	-2.15	9.87E-05	1.68E-02
RBBP8	Retinoblastoma b.p 8	-2.15	5.02E-05	1.25E-02
RNU6-57P	RNA, U6 small nuclear 57, pseudogene	-2.15	4.00E-04	3.80E-02
ANLN	Anillin actin b.p	-2.16	8.51E-05	1.55E-02
FIGN	Fidgetin	-2.16	2.00E-04	2.14E-02
GSG2	Germ cell associated 2 (haspin)	-2.16	1.00E-04	1.89E-02
HIST1H3B	Histone cluster 1, H3b	-2.16	4.24E-05	1.16E-02
CDC25A	Cell division cycle 25A	-2.18	3.00E-04	3.16E-02
CCNB2	Cyclin B2	-2.18	2.00E-04	2.48E-02
G2E3	G2/M-phase specific E3 ubiquitin protein ligase	-2.18	6.00E-04	4.94E-02
KIF14	Kinesin fam. mem. 14	-2.18	2.00E-04	2.56E-02
TMPO	Thymopoietin	-2.18	4.43E-05	1.17E-02
PAK6; BUB1B	p21 protein (Cdc42/Rac)-Activated kinase 6; BUB1	-2.19	4.23E-05	1.16E-02
RFC3	Replication factor C su. 3	-2.19	1.70E-05	7.50E-03
CCNE2	Cyclin E2	-2.20	7.59E-06	5.70E-03
PSIP1	PC4 and SFRS1 interacting protein 1	-2.20	6.44E-05	1.36E-02

Table I. *Continued*

Table I. *Continued*

Gene symbol	Description	Fold change	*p*-Value	FDR *p*-Value
RBL1	Retinoblastoma-like 1	-2.20	2.00E-04	2.15E-02
SMC4	Structural maintenance of chromosomes 4	-2.20	2.14E-05	8.20E-03
XRCC2	X-ray repair cdr in Chinese hamster cells 2	-2.20	9.50E-05	1.65E-02
FANCI	Fanconi anemia complementation group I	-2.21	1.00E-04	1.80E-02
FAM216A	Fam. with sequence similarity 216, mem. A	-2.22	3.00E-04	3.26E-02
HELLS	Helicase, lymphoid-specific	-2.22	2.99E-05	9.80E-03
NEK2	NIMA-related kinase 2	-2.22	3.00E-04	3.29E-02
NCAPG	Non-SMC condensin I complex su. G	-2.22	5.94E-05	1.32E-02
NCAPH	Non-SMC condensin I complex su. H	-2.22	1.45E-05	7.40E-03
SDPR	Serum deprivation response	-2.22	1.00E-04	1.87E-02
UBE2C	Ubiquitin-conjugating enzyme E2C	-2.22	1.00E-04	2.05E-02
LOC100507516	Uncharacterized LOC100507516	-2.22	2.00E-04	2.44E-02
CIT; MIR1178	Citron rho-interacting Ser/thrkinase; microRNA 1178	-2.23	2.78E-05	9.70E-03
CENPI	Centromere protein I	-2.24	4.00E-04	3.62E-02
GINS1	GINS complex su. 1 (Psf1 homolog)	-2.24	1.91E-05	7.90E-03
GINS4	GINS complex su. 4 (Sld5 homolog)	-2.25	5.88E-06	5.30E-03
KIF20B	Kinesin fam. mem. 20B	-2.25	3.00E-04	3.08E-02
HIST2H2AB	Histone cluster 2, H2ab	-2.26	1.27E-05	6.90E-03
SLFN13	Schlafen fam. mem. 13	-2.26	3.54E-05	1.05E-02
UBE2T	Ubiquitin conjugating enzyme E2T	-2.26	2.40E-06	3.20E-03
PCNA-AS1	PCNA antisense RNA 1	-2.27	7.19E-05	1.42E-02
TIMELESS	Timeless circadian clock	-2.27	6.12E-05	1.33E-02
MMS22L	MMS22-like, DNA repair protein	-2.29	2.94E-05	9.70E-03
PARPBP	PARP1 b.p	-2.29	3.00E-04	3.03E-02
C18orf54	Chromosome 18 open reading frame 54	-2.30	9.02E-05	1.60E-02
CCDC138	Coiled-coil d.c. 138	-2.30	6.00E-04	4.55E-02
MKI67	Marker of proliferation Ki-67	-2.30	1.14E-05	6.50E-03
VRK1; LINC00618	Vaccinia related kinase 1; LIN RNA 618	-2.30	1.00E-04	1.81E-02
ZNF215	Zinc finger protein 215	-2.30	2.63E-05	9.30E-03
GMNN	Geminin, DNA replication inhibitor	-2.31	5.80E-05	1.31E-02
NUSAP1	Nucleolar and spindle associated protein 1	-2.31	3.97E-05	1.13E-02
CCNB1	Cyclin B1	-2.32	5.24E-05	1.27E-02
RAD54L	RAD54-like (S. cerevisiae)	-2.32	5.00E-04	4.16E-02
ARHGAP11A	Rho GTPase activating protein 11A	-2.32	3.16E-05	1.00E-02
TMPO-AS1	TMPO antisense RNA 1	-2.32	5.44E-06	5.10E-03
ASPM	Aabnormal spindle microtubule assembly	-2.33	2.00E-04	2.17E-02
ATAD2	ATPase fam., AAA d.c. 2	-2.34	7.06E-05	1.41E-02
FOXM1	Forkhead box M1	-2.34	8.37E-05	1.53E-02
FIGNL1	Fidgetin-like 1	-2.35	3.79E-05	1.09E-02
LOC105376603	Uncharacterized LOC105376603	-2.35	6.61E-05	1.37E-02
C1orf112	Chromosome 1 open reading frame 112	-2.36	2.91E-05	9.70E-03
KIF18B	Kinesin fam. mem. 18B	-2.36	3.59E-05	1.05E-02
BLM	Bloom syndrome, RecQ helicase-like	-2.37	4.97E-05	1.25E-02
KIF4A	Kinesin fam. mem. 4A	-2.39	5.00E-04	4.24E-02
MND1	Meiotic nuclear divisions 1	-2.39	1.30E-05	6.90E-03
NUF2	NUF2, NDC80 kinetochore complex component	-2.39	5.00E-04	4.01E-02
C5orf34	Chromosome 5 open reading frame 34	-2.40	5.60E-05	1.30E-02
CDKN3	cyclin-dependent kinase inhibitor 3	-2.41	9.46E-05	1.65E-02
FANCD2	Fanconi anemia complementation group D2	-2.41	7.18E-05	1.42E-02
PLK4	Polo-like kinase 4	-2.41	2.00E-04	2.17E-02
BARD1	BRCA1 associated RING domain 1	-2.44	1.44E-05	7.40E-03
CENPE	Centromere protein E	-2.44	4.00E-04	3.42E-02
MAD2L1	MAD2 mitotic arrest deficient-like 1 (yeast)	-2.44	2.00E-04	2.17E-02
SHCBP1	SHC SH2-domain b.p 1	-2.45	1.10E-05	6.50E-03
WDR76	WD repeat domain 76	-2.45	1.00E-04	1.83E-02
FBXO43	F-box protein 43	-2.46	4.96E-05	1.25E-02
CDC6	Cell division cycle 6	-2.47	2.00E-04	2.61E-02
ESPL1	Extra spindle pole bodies like 1, separase	-2.47	5.09E-05	1.26E-02

Table I. *Continued*

Table I. *Continued*

Gene symbol	Description	Fold change	*p*-Value	FDR *p*-Value
DEPDC1B	DEP d.c. 1B	-2.48	1.00E-04	2.00E-02
HMMR	Hyaluronan-mediated motility receptor (RHAMM)	-2.48	3.00E-04	3.09E-02
KIFC1	Kinesin fam. mem. C1	-2.48	3.34E-05	1.04E-02
RAD51AP1	RAD51 associated protein 1	-2.48	1.00E-04	1.69E-02
SPC24	SPC24, NDC80 kinetochore complex component	-2.48	7.12E-06	5.70E-03
CENPU	Centromere protein U	-2.49	1.50E-05	7.40E-03
KIF11	Kinesin fam. mem. 11	-2.49	3.63E-05	1.06E-02
NEIL3	Nei-like DNA glycosylase 3	-2.49	8.28E-06	5.90E-03
FBXO5	F-box protein 5	-2.50	2.00E-04	2.48E-02
KIF2C	Kinesin fam. mem. 2C	-2.50	1.06E-05	6.30E-03
CEP295	Centrosomal protein 295kDa	-2.51	1.00E-04	1.81E-02
TOP2A	Topoisomerase (DNA) II alpha	-2.51	6.59E-05	1.37E-02
SUV39H2	Suppressor of variegation 3-9 homolog 2 (Drosophila)	-2.52	2.00E-04	2.37E-02
ARHGAP11B	Rho GTPase activating protein 11B	-2.54	1.05E-05	6.30E-03
DLGAP5	Discs, large (Drosophila) homolog-associated protein 5	-2.55	1.00E-04	1.89E-02
HMGN2	High mobility group nucleosomal binding domain 2	-2.55	1.00E-04	1.81E-02
ZGRF1	Zinc finger, GRF-type containing 1	-2.55	2.65E-05	9.30E-03
TRIP13	Thyroid hormone receptor interactor 13	-2.57	1.00E-04	1.93E-02
BRIP1	BRCA1 interacting protein C-terminal helicase 1	-2.59	1.67E-05	7.50E-03
BUB1	BUB1 mitotic checkpoint serine/threonine kinase	-2.59	2.01E-05	8.00E-03
ESCO2	Establishment of sister chromatid c.N-acetyltransferase 2	-2.61	1.93E-06	3.00E-03
GEN1	GEN1 Holliday junction 5 flap endonuclease	-2.61	6.76E-05	1.39E-02
SPC25	SPC25, NDC80 kinetochore complex component	-2.61	9.19E-06	6.00E-03
TACC3	Transforming, acidic coiled-coil containing protein 3	-2.61	4.29E-06	4.60E-03
DEPDC1	DEP d.c. 1	-2.62	3.00E-04	2.99E-02
HJURP	Holliday junction recognition protein	-2.63	3.58E-06	4.40E-03
EXO1	Exonuclease 1	-2.65	1.92E-05	7.90E-03
KIF18A	Kinesin fam. mem. 18A	-2.65	8.64E-05	1.56E-02
KIAA1524	KIAA1524	-2.67	2.00E-04	2.65E-02
LMNB1	Lamin B1	-2.67	2.37E-05	8.60E-03
CDK1	Cyclin-dependent kinase 1	-2.68	7.24E-05	1.42E-02
SERTAD4	SERTA d.c. 4	-2.68	4.00E-04	3.72E-02
MCM10	MCM 10 replication initiation factor	-2.70	1.66E-05	7.50E-03
KIF15	Kinesin fam. mem. 15	-2.71	9.35E-06	6.00E-03
KIF20A	Kinesin fam. mem. 20A	-2.73	1.81E-05	7.80E-03
POLE2	Polymerase (DNA directed), epsilon 2, accessory su.	-2.75	9.01E-07	2.30E-03
OIP5	Opa interacting protein 5	-2.77	2.00E-05	8.00E-03
SKA3	Spindle and kinetochore Associated complex su. 3	-2.77	9.33E-06	6.00E-03
CDCA7	Cell division cycle associated 7	-2.78	6.94E-06	5.70E-03
DNA2	DNA replication Helicase/nuclease 2	-2.79	1.71E-05	7.50E-03
NDC80	NDC80 kinetochore complex component	-2.82	1.00E-04	1.73E-02
CENPK	Centromere protein K	-2.83	1.48E-05	7.40E-03
CDC7	Cell division cycle 7	-2.86	1.61E-06	2.80E-03
ATAD5	ATPase fam., AAA d.c. 5	-2.87	1.15E-05	6.50E-03
FANCM	Fanconi anemia complementation group M	-2.88	1.23E-05	6.80E-03
FAM111B	Fam. with sequence similarity 111, mem. B	-2.89	1.68E-06	2.80E-03
PBK	PDZ binding kinase	-2.89	4.74E-05	1.22E-02
CCNA2	Cyclin A2	-2.91	5.24E-06	5.10E-03
SGOL1-AS1	SGOL1 antisense RNA 1	-2.92	1.00E-04	1.80E-02
BRCA2	Breast cancer 2, early onset	-2.94	6.66E-05	1.37E-02
CDCA2	Cell division cycle associated 2	-3.00	8.82E-06	6.00E-03
PRIM1	Primase, DNA, polypeptide 1 (49kDa)	-3.01	6.46E-07	2.10E-03
CDCA8	Cell division cycle associated 8	-3.06	1.63E-06	2.80E-03
GPX8	Glutathione peroxidase 8 (putative)	-3.17	6.00E-04	4.93E-02
FAM83D	Fam. with sequence similarity 83, mem. D	-3.20	2.77E-06	3.50E-03
POLQ	Polymerase (DNA directed), theta	-3.30	1.00E-04	1.70E-02
BORA	Bora, aurora kinase A activator	-3.53	4.12E-05	1.16E-02
DSCC1	DNA replication and sister chromatid cohesion 1	-3.60	2.02E-06	3.00E-03
SGOL1	Shugoshin-like 1 (S. pombe)	-3.61	1.29E-05	6.90E-03
MIR924	MicroRNA 924	-3.68	2.00E-04	2.17E-02

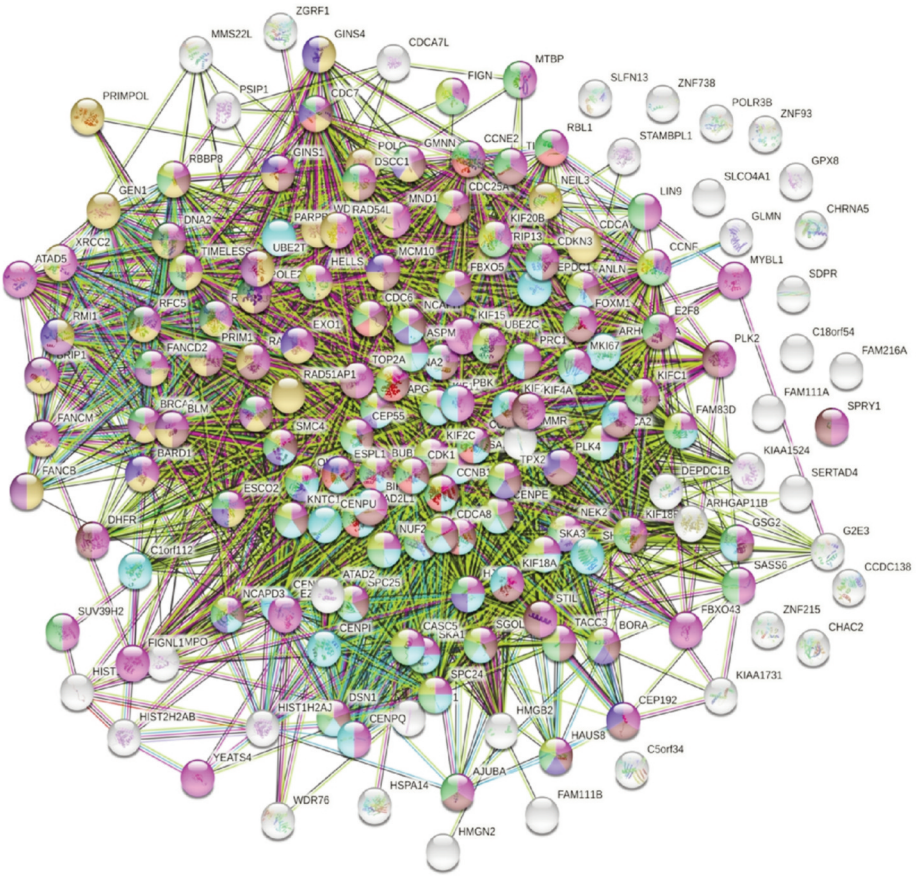

ID	Go-Term	Description	Count in Network	Strength	FDR	Color Code
		Biological Process (Gene Ontology)				
Go Term	GO:1903047	Mitotic Cell Cycle Process	70 of 564	1.16	7.653-57	
Go Term	GO:00007049	Cell cycle	11 of 1263	1.01	2.35E-83	
		Cellular Component (Gene Ontology)				
Go Term	GO:0005694	Chromosome	74 of 950	0.96	2.13E-47	
Go Term	GO:0000775	Chromosome Centromeric Region	34 of 189	1.32	4.90E-31	
		Local Network Cluster (STRING)				
Cluster	CL:12167	Kinectichore / Chromosome	51 of 123	1.68	4.48E-63	
Cluster	CL:12605	DNA Replication, Interstsrand cross-link repair	39 of 184	1.39	1.86E-38	
		Kegg Pathways				
Pathway	hsa-04110	Cell Cycle	13 of 123	1.09	8.95E-09	
Pathway	hsa-03460	Fanconi anemia pathway	9 of 51	1.31	5.59E-08	
Pathway	hsa-03030	DNA Replication	5 of 36	1.21	2.00E-04	
		Reactome Pathway				
Pathway	HSA-1640170	Cell Cycle	23 of 160	1.22	6.80E-19	
		Annotated Keywords (UniProt)				
Keyword	KW-0131	Cell Cycle	72 of 640	1.11	1.70E-56	
Keyword	KW-0498	Mitosis	49 of 268	1.33	4.11E-46	

Figure 5. *Stringdb relational network analysis of down-regulated DEGS caused by WYE (Low) 15 μg/ml vs. untreated controls after meeting selection criteria; -2<x>+2 fold change, p-Value <0.05 and FDR p-Value <0.05. The data in the corresponding table: represent database used, ID #s within a database, description of system altered, count in the network for system, strength of relationship and the false discovery rate (FDR) p-Value. Color codes indicate genes (by symbol) in the string diagram corresponding to the table class description.*

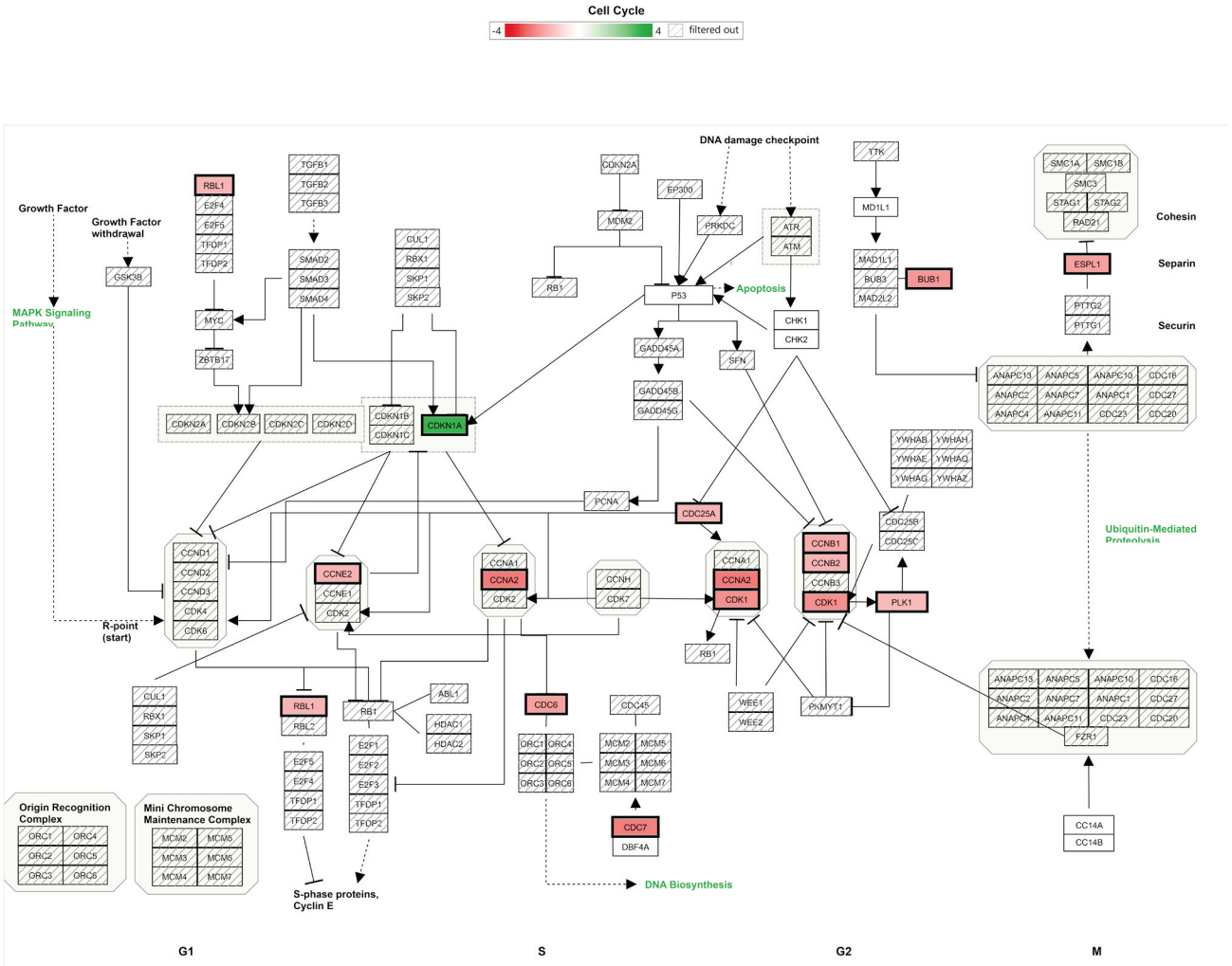

Figure 6. *Cell cycle Wikipathway analysis report for DEGS caused by WYE (Low) 15 μg/ml vs. untreated controls after meeting selection criteria; -2<x>+2, p-Value <0.05 and FDR p-Value <0.05. DEGS are color coded (red=down), (green=up) with color intensity darker with fold higher fold change. Gene symbol denoted by cross bars /// were not altered.*

To our knowledge, this is the first scientific report describing the pro-inflammatory immune-stimulating properties of WYE in a cancer cell line, amongst what appears to be an absence in the literature of similar type studies. Meanwhile, for over 60 years, the research literature has been well established for describing the effects of low-dose saponins as immune-stimulating vaccine adjuvants, which carry out the sole purpose of stimulating a strong, long-lasting learned immune response to administered vaccine antigens. Saponin adjuvants bear a similar molecular similarity to known saponins in WYE, some of which include Quil A, QS-21 from *Quillaja*, and saponins in the *Momordica* (35), *Glycyrrhiza* (36), and the *Dioscorea* botanical species itself (37). Botanically derived saponin adjuvants boost the immune system by increasing the Th1/Th2 cell-mediated response, antibody production, targeted cytotoxic T-CD4+ cell response with concurrent stimulation of a variety of cytokines [IL-2, IL-10, IL-12 (p70) and IFN-γ] (20, 38-44). Yet, interestingly, most of all of the studies on saponin adjuvants have been carried out only in the presence of the antigenic substance containing the vaccine. To add to this gap in the literature, only a few studies have explored the immune-stimulating properties of saponin-rich herbs, which describe an effect on the innate immune response by crude extracts or compounds within *Dioscorea* species. These changes include capacity to stimulate phagocytosis in macrophages, enhance natural killer (NK) cell activity, activate Toll-like receptor 4 (TLR4) and activate downstream

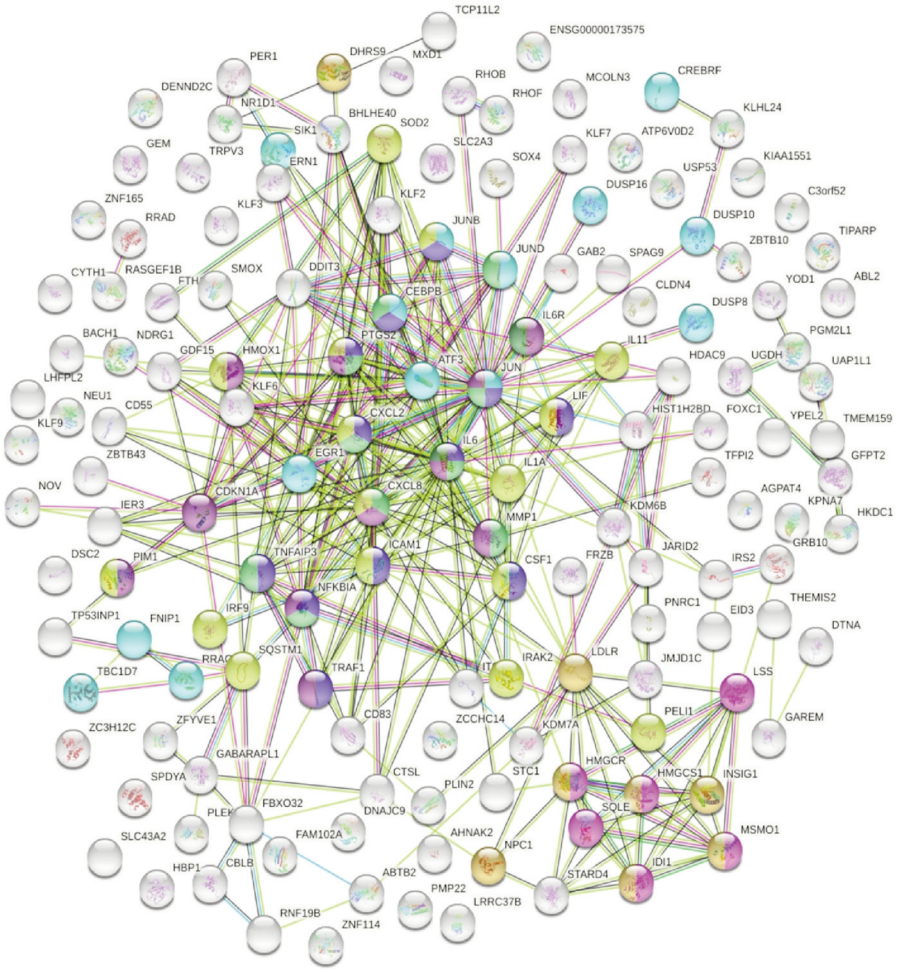

ID	Go-Term	Description	Count in Network	Strength	FDR	Color Code
		Annotated Keywords (UniProt)				
Keyword	KW-0753	Steroid Metabolism	8 of 96	1.05	2.20E-05	
		Local network cluster (STRING)				
Cluster	CL: 2190	Regulation of TOR Signaling/ MAPK targets	14 of 196	0.98	2.62E-07	
Cluster	CL: 23466	Cholesterol Biosynthesis	6 of 17	1.68	2.14E-06	
Cluster	CL:2482	AP-1 transcription factor, and JUN	5 of 12	1.75	9.59E-06	
Cluster	CL: 23468	Steroid Biosynthesis	3 of 6	1.83	1.10E-03	
		KEGG Pathways				
Pathway	hsa04657	IL-17 Signaling pathway	10 of 92	1.17	2.41E-07	
Pathway	hsa05200	Pathways in Cancer	11 of 515	0.46	1.12E-02	
Pathway	hsa04668	TNF signaling pathway	12 of 108	1.18	1.48E-08	
		Reactome Pathways				
Pathway	hsa-1280215	Cytokine Signaling in Immune System	16 of 328	0.82	1.74E-07	
Pathway	hsa-1059683	Interleukin-6 Signaling	2 of 11	1.39	2.62E-02	

Figure 7. *Stringdb relational network analysis of up-regulated DEGS caused by WYE (Low) 15 μg/mL vs. untreated controls after meeting selection criteria; -2<x>+2, p-Value <0.05 and FDR p-Value <0.05. The data represent database used, ID #s within a database, description of system altered, count in the network for system, strength of relationship and the false discovery rate (FDR) p-Value. Color codes indicate genes (by symbol) in the string diagram corresponding to the table class description.*

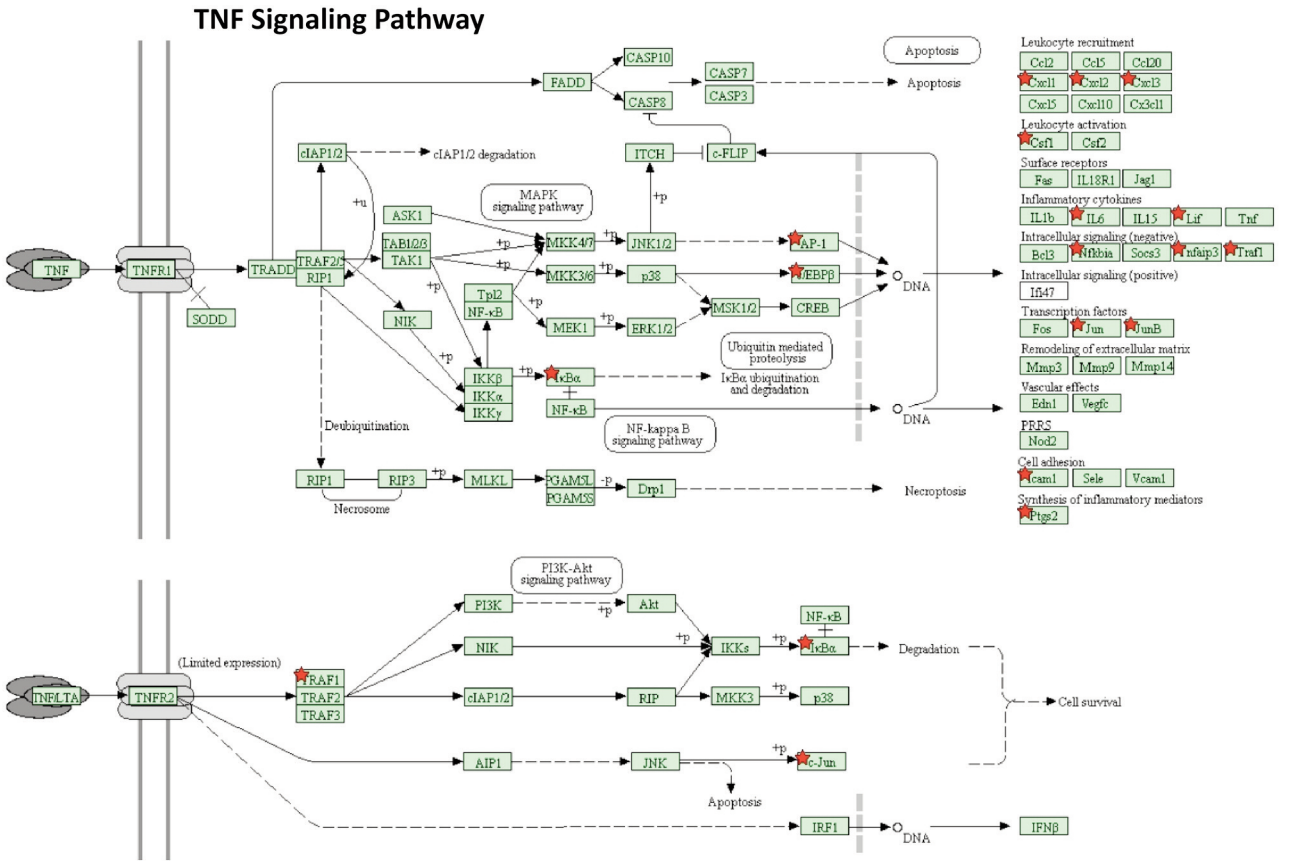

Figure 8. *TNF signaling Kegg Pathway report for up-regulated DEGS caused by WYE (Low) 15 μg/ml vs. untreated controls after meeting selection criteria; -2<x>+2 fold change, p-Value <0.05 and FDR p-Value <0.05. Up-regulated DEGS are demarcated by a red star.*

signaling pathways (ERK/JNK, and p38) involving cytokine release (*e.g.*, IL-2, IFN-γ, TNF-α, IL-1b, and IL-6) (45-47). Similarly, *Dioscorea* glycoproteins alone can trigger infiltration and recruitment of macrophages, lymphocytes, neutrophils, and monocytes while at the same time augmenting NK cytotoxic cell response (48, 49). There is some remote similarity in the manner in which biological responses to the FDA approved saponin adjuvant used for the zoster vaccine (50) AS01 (the QS-21 saponin) works to activate the immune system, such as acting on TLR4 signaling, however, reports central around activation of the adaptive immune response (38, 51-53). In turn, there are also studies showing that other types of saponin-rich plants can stimulate both the innate and adaptive immune response by activation of TLR4, NK cells, humoral and cell-mediated immunity, macrophage phagocytosis, cytokine and immunoglobulin production, and T CD8+ cell-mediated anticancer immune response, such as the case for *Codonopsis pilosula* (54, 55) and *Astragalus* (56-58).

While data in this work show WYE to evoke some immune response in the cancer cells itself, the impact of this remains speculative. We cannot exclude the possibility that it could also worsen existing cancers with an inflammatory component. In brief, the immune system is a double-edged sword as it plays a role in both the destruction of/and pathological advancement of cancer. Initiation of cancer can occur from many injurious environmental elements, including; chronic persistent inflammation, exposure to pathogens, irritants, toxins with greater vulnerability occurring in immunocompromised individuals. There is a delicate balance between immunosuppression (under-active) and inflammation (over-active) which controls the initial susceptibility to cancer and various infections.

A healthy immune system will recognize and destroy malignant cells on demand. In established cancers, the host immune system no longer recognizes malignant cells (immune escape) but instead supports the survival,

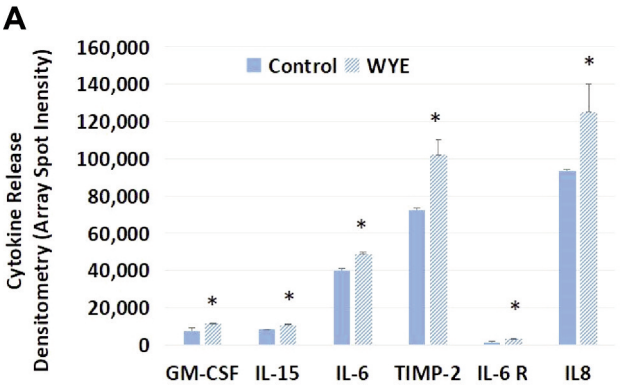

B

mRNA Microarray Values (Control vs. WYE Low)

Gene Symbol	Description	Fold Change	*p*-Value	FDR *p*-Value
CSF2	colony stimulating factor 2 (granulocyte-macrophage)	1.57	0.005	1.67E-01
IL15	interleukin 15	1.26	0.017	3.08E-01
IL6	interleukin 6	2.23	<0.001	2.16E-02
TIMP2; CEP295NL	TIMP metallopeptidase inhibitor 2; CEP295 N-terminal like	1.52	0.002	9.41E-02
IL6R	interleukin 6 receptor	2.39	<0.001	1.81E-02
CXCL8	chemokine (C-X-C motif) ligand 8	9.09	<0.001	1.83E-05

Figure 9. *Supernatant cytokine detection vs. mRNA transcript. Cytokine released in untreated controls vs. (WYE-Low, 15 µg/ml) in supernatants obtained from the same pellets used for microarray analysis and analyzed by a human cytokine array. The data represents matched changes occurring in both the protein antibody with *p-Values <0.05 in both sets, where array values were set at selection criteria; any fold change, p-Value <0.05 and no filter on FDR p-Values (B). There was a high degree of matching values between proteins released in the supernatant and the mRNA produced for those proteins.*

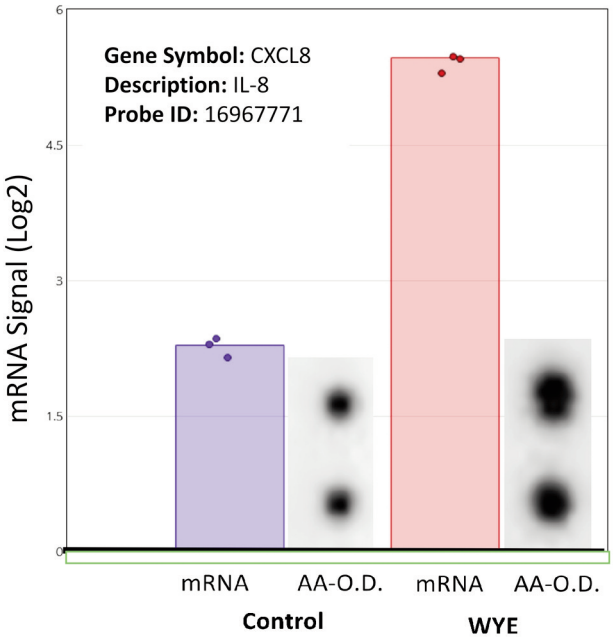

Figure 10. *Supernatant cytokine detection. Supernatants collected from pellets used for microarray analysis (WYE-Low, 15ug/ml) show semi-quantitative changes in IL-8 by anti-body array (densitometry spot duplicates), demarcated alongside transcriptomic microarray chip spot probe arrays for IL-8 in MDA-MB-231 cells.*

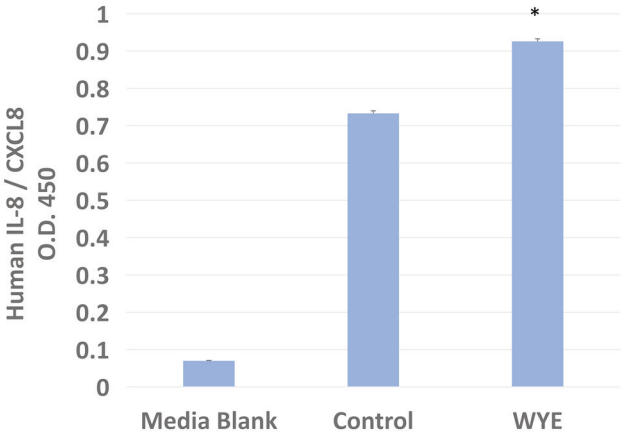

Figure 11. *Supernatants collected from pellets used for microarray analysis (WYE-Low, 15 µg/ml) show quantitative changes in IL-8 as determined by ELISA. The data represent the mean±S.E.M for optical densitometry values, n=3 and significant differences between the control and treatment was determined by a students t-test; *p<0.05.*

proliferation, and metastasis of cancer. This is carried out by the formation of a protective inflammatory barrier within the tumor microenvironment (TME) (59, 60) which fosters cancer growth while at the same time suppresses the body's immune system to recognize and target cancer (61). The elevation of cytokines released by the tumor tissue itself could worsen pre-existing cancers, driving inward trafficking of leukocyte subpopulations such as monocytes toward the tumor (62), which along with acidity, can polarize and mature into M2- tumor-associated macrophages (TAMS) (63, 64). The M2 tumor-promoting phenotype is largely immunosuppressive, aligning with the increased presence of cytokines (IL-6, IL-8, IL-10), COX2, cathepsins, IL-1A, and MMPS within the TME, creating a highly inflammatory aggressive breast cancer with poor clinical outcome (65-72). In the current work, we showed that WYE at very low concentrations, in theory, could perpetuate the M2 phenotype by establishing

tumor cell production of COX2, and the release of cathepsins, MMP1, IL-8, IL-6, IL-1A, and CCL2, the consequences of which would be counter-indicated and harmful for cancer patients.

While on the one hand, the WYE used in this study provokes a rise in aggravating tumor cytokines, paradoxically compounds in the *Dioscorea* species are known to augment the body's natural capacity to target and destroy tumor cells, as described above. The ability to redirect the body to destroy its own tumor cells is the aim of current-day research in developing immune-modulating anticancer drugs. These therapies aim to restore the body's natural immune killing capacity by a) penetrating through the TME and b) activating tumor recognition and destruction by the body's tumor CD8+ T cytotoxic and NK. Cells, both being used in adoptive immune therapies (AIT) (73, 74). While there are most certainly natural compounds unidentified to date that can do this, at the current time, AITs involves using the patient's blood to derive peripheral blood mononuclear cells (PBMCs), which are genetically engineered or modified then reinfused back into the same patient to target cancer (59, 75). However, it would suffice to say that any agent, drug, or process can mimic the effect of AITs to boost the body's own NK cells (76) cytotoxic T (CD8+)/ Th (CD4+), antigen-presenting dendritic cells (DCs)/cytokine-induced killer (CIK) cells (DC-CIK cells therapies) (77-79) would, in theory, establish long term immunity and positive patient outcome including for individuals with stage IV breast and TNBC cancers (80-83).

In conclusion, this work provides an overall transcriptomic analysis of WYE at sub-lethal concentrations, corroborating existing evidence by demonstrating its cytostatic effects and establishing a unique immune-stimulatory response. This work emphasizes the need for future research to investigate the immune stimulatory effects of saponin-rich herbs as it relates to cancer prevention and/or treatment.

Availability of Data and Material

The dataset has been deposited to NIH. Gene Expression Omnibus located at: https://www.ncbi.nlm.nih.gov/geo/query/acc.cgi?acc=GSE180621.

Conflicts of Interest

The Authors declare that they have no conflicts of interest.

Authors' Contributions

EM and AA conducted studies on cell viability, saponins, antibody arrays, ELISA, and microarray. SDR and KS were involved with troubleshooting, literature review, manuscript preparation, and KS oversaw and guided this project.

Acknowledgements

This research was supported by the National Institute of Minority Health and Health Disparities of the National Institutes of Health through Grant Number U54 MD 007582 and Grant Number P20 MD 006738

References

1 Park MK, Kwon HY, Ahn WS, Bae S, Rhyu MR and Lee Y: Estrogen activities and the cellular effects of natural progesterone from wild yam extract in mcf-7 human breast cancer cells. Am J Chin Med *37(1)*: 159-167, 2009. PMID: 19222119. DOI: 10.1142/S0192415X09006746

2 Aumsuwan P, Khan SI, Khan IA, Avula B, Walker LA, Helferich WG, Katzenellenbogen BS and Dasmahapatra AK: Evaluation of wild yam (*Dioscorea villosa*) root extract as a potential epigenetic agent in breast cancer cells. In Vitro Cell Dev Biol Anim *51(1)*: 59-71, 2015. PMID: 25148825. DOI: 10.1007/s11626-014-9807-5

3 Depypere HT and Comhaire FH: Herbal preparations for the menopause: beyond isoflavones and black cohosh. Maturitas *77(2)*: 191-194, 2014. PMID: 24314619. DOI: 10.1016/j.maturitas.2013.11.001

4 Mazzio E, Badisa R, Mack N, Deiab S and Soliman KF: High throughput screening of natural products for anti-mitotic effects in MDA-MB-231 human breast carcinoma cells. Phytother Res *28(6)*: 856-867, 2014. PMID: 24105850. DOI: 10.1002/ptr.5065

5 Chiang CT, Way TD, Tsai SJ and Lin JK: Diosgenin, a naturally occurring steroid, suppresses fatty acid synthase expression in HER2-overexpressing breast cancer cells through modulating Akt, mTOR and JNK phosphorylation. FEBS Lett *581(30)*: 5735-5742, 2007. PMID: 18022396. DOI: 10.1016/j.febslet.2007.11.021

6 Salehi B, Sener B, Kilic M, Sharifi-Rad J, Naz R, Yousaf Z, Mudau FN, Fokou PVT, Ezzat SM, El Bishbishy MH, Taheri Y, Lucariello G, Durazzo A, Lucarini M, Suleria HAR and Santini A: *Dioscorea* plants: A genus rich in vital nutra-pharmaceuticals-a review. Iran J Pharm Res *18(Suppl1)*: 68-89, 2019. PMID: 32802090. DOI: 10.22037/ijpr.2019.112501.13795

7 He Z, Chen H, Li G, Zhu H, Gao Y, Zhang L and Sun J: Diosgenin inhibits the migration of human breast cancer MDA-MB-231 cells by suppressing Vav2 activity. Phytomedicine *21(6)*: 871-876, 2014. PMID: 24656238. DOI: 10.1016/j.phymed.2014.02.002

8 Bhuvanalakshmi G, Basappa, Rangappa KS, Dharmarajan A, Sethi G, Kumar AP and Warrier S: Breast cancer stem-like cells are inhibited by diosgenin, a steroidal saponin, by the attenuation of the Wnt β-catenin signaling via the Wnt antagonist secreted frizzled related protein-4. Front Pharmacol *8*: 124, 2017. PMID: 28373842. DOI: 10.3389/fphar.2017.00124

9 Zhao J, Xu Y, Wang C, Ding Y, Chen M, Wang Y, Peng J, Li L and Lv L: Soluplus/TPGS mixed micelles for dioscin delivery in cancer therapy. Drug Dev Ind Pharm *43(7)*: 1197-1204, 2017. PMID: 28300426. DOI: 10.1080/03639045.2017.1304956

10 Liao WL, Lin JY, Shieh JC, Yeh HF, Hsieh YH, Cheng YC, Lee HJ, Shen CY and Cheng CW: Induction of G2/M phase arrest by diosgenin *via* activation of Chk1 kinase and Cdc25C regulatory pathways to promote apoptosis in human breast cancer cells. Int J Mol Sci *21(1)*: 172, 2019. PMID: 31881805. DOI: 10.3390/ijms21010172

11 Masood-Ur-Rahman, Mohammad Y, Fazili KM, Bhat KA and Ara T: Synthesis and biological evaluation of novel 3-O-tethered triazoles of diosgenin as potent antiproliferative agents. Steroids *118*: 1-8, 2017. PMID: 27864018. DOI: 10.1016/j.steroids.2016.11.003

12 Yeager JF: Hemolysis by saponin and sodium taurocholate, with special reference to the series of Ryvosh. J Gen Physiol *11(6)*: 779-787, 1928. PMID: 19872434. DOI: 10.1085/jgp.11.6.779

13 Efimova SS and Ostroumova OS: Is the membrane lipid matrix a key target for action of pharmacologically active plant saponins? Int J Mol Sci *22(6)*: 3167, 2021. PMID: 33804648. DOI: 10.3390/ijms22063167

14 Orczyk M, Wojciechowski K and Brezesinski G: The influence of steroidal and triterpenoid saponins on monolayer models of the outer leaflets of human erythrocytes, E. coli and S. cerevisiae cell membranes. J Colloid Interface Sci *563*: 207-217, 2020. PMID: 31874308. DOI: 10.1016/j.jcis.2019.12.014

15 Malabed R, Hanashima S, Murata M and Sakurai K: Interactions of OSW-1 with lipid bilayers in comparison with digitonin and soyasaponin. Langmuir *36(13)*: 3600-3610, 2020. PMID: 32160747. DOI: 10.1021/acs.langmuir.9b03957

16 Verstraeten SL, Albert M, Paquot A, Muccioli GG, Tyteca D and Mingeot-Leclercq MP: Membrane cholesterol delays cellular apoptosis induced by ginsenoside Rh2, a steroid saponin. Toxicol Appl Pharmacol *352*: 59-67, 2018. PMID: 29782965. DOI: 10.1016/j.taap.2018.05.014

17 Chen M, Balhara V, Jaimes Castillo AM, Balsevich J and Johnston LJ: Interaction of saponin 1688 with phase separated lipid bilayers. Biochim Biophys Acta Biomembr *1859(7)*: 1263-1272, 2017. PMID: 28389202. DOI: 10.1016/j.bbamem.2017.03.024

18 Xu XH, Li T, Fong CM, Chen X, Chen XJ, Wang YT, Huang MQ and Lu JJ: Saponins from Chinese medicines as anticancer agents. Molecules *21(10)*: 1326, 2016. PMID: 27782048. DOI: 10.3390/molecules21101326

19 Sudji IR, Subburaj Y, Frenkel N, García-Sáez AJ and Wink M: Membrane disintegration caused by the steroid saponin digitonin is related to the presence of cholesterol. Molecules *20(11)*: 20146-20160, 2015. PMID: 26569199. DOI: 10.3390/molecules201119682

20 Lacaille-Dubois MA and Wagner H: A review of the biological and pharmacological activities of saponins. Phytomedicine *2(4)*: 363-386, 1996. PMID: 23194774. DOI: 10.1016/S0944-7113(96)80081-X

21 Koczurkiewicz P, Klaś K, Grabowska K, Piska K, Rogowska K, Wójcik-Pszczoła K, Podolak I, Galanty A, Michalik M and Pękala E: Saponins as chemosensitizing substances that improve effectiveness and selectivity of anticancer drug-Minireview of *in vitro* studies. Phytother Res *33(9)*: 2141-2151, 2019. PMID: 31294509. DOI: 10.1002/ptr.6371

22 Tong QY, He Y, Zhao QB, Qing Y, Huang W and Wu XH: Cytotoxicity and apoptosis-inducing effect of steroidal saponins from *Dioscorea* zingiberensis Wright against cancer cells. Steroids *77(12)*: 1219-1227, 2012. PMID: 22575181. DOI: 10.1016/j.steroids.2012.04.019

23 Jaiaree N, Itharat A and Kumapava K: Cytotoxic saponin against lung cancer cells from *Dioscorea* birmanica Prain & Burkill. J Med Assoc Thai *93(Suppl 7)*: S192-S197, 2010. PMID: 21294414.

24 Schneider CA, Rasband WS and Eliceiri KW: NIH Image to ImageJ: 25 years of image analysis. Nat Methods *9(7)*: 671-675, 2012. PMID: 22930834. DOI: 10.1038/nmeth.2089

25 Jones KH and Senft JA: An improved method to determine cell viability by simultaneous staining with fluorescein diacetate-propidium iodide. J Histochem Cytochem *33(1)*: 77-79, 1985. PMID: 2578146. DOI: 10.1177/33.1.2578146

26 Crowley LC, Christensen ME and Waterhouse NJ: Measuring mitochondrial transmembrane potential by TMRE staining. Cold Spring Harb Protoc *2016(12)*, 2016. PMID: 27934682. DOI: 10.1101/pdb.prot087361

27 McMillian MK, Li L, Parker JB, Patel L, Zhong Z, Gunnett JW, Powers WJ and Johnson MD: An improved resazurin-based cytotoxicity assay for hepatic cells. Cell Biol Toxicol *18(3)*: 157-173, 2002. PMID: 12083422. DOI: 10.1023/a:1015559603643

28 Szklarczyk D, Franceschini A, Kuhn M, Simonovic M, Roth A, Minguez P, Doerks T, Stark M, Muller J, Bork P, Jensen LJ and von Mering C: The STRING database in 2011: functional interaction networks of proteins, globally integrated and scored. Nucleic Acids Res *39(Database issue)*: D561-D568, 2011. PMID: 21045058. DOI: 10.1093/nar/gkq973

29 Szklarczyk D, Gable AL, Nastou KC, Lyon D, Kirsch R, Pyysalo S, Doncheva NT, Legeay M, Fang T, Bork P, Jensen LJ and von Mering C: The STRING database in 2021: customizable protein-protein networks, and functional characterization of user-uploaded gene/measurement sets. Nucleic Acids Res *49(D1)*: D605-D612, 2021. PMID: 33237311. DOI: 10.1093/nar/gkaa1074

30 Huang DW, Sherman BT, Tan Q, Collins JR, Alvord WG, Roayaei J, Stephens R, Baseler MW, Lane HC and Lempicki RA: The DAVID Gene Functional Classification Tool: a novel biological module-centric algorithm to functionally analyze large gene lists. Genome Biol *8(9)*: R183, 2007. PMID: 17784955. DOI: 10.1186/gb-2007-8-9-r183

31 Duangprompo W, Aree K, Itharat A and Hansakul P: Effects of 5,6-dihydroxy-2,4-dimethoxy-9,10-dihydrophenanthrene on G_2/M cell cycle arrest and apoptosis in human lung carcinoma cells. Am J Chin Med *44(7)*: 1473-1490, 2016. PMID: 27776429. DOI: 10.1142/S0192415X16500828

32 Xie YL, Fan M, Jiang RM, Wang ZL and Li Y: Deltonin induced both apoptosis and autophagy in head and neck squamous carcinoma FaDu cell. Neoplasma *62(3)*: 419-431, 2015. PMID: 25866222. DOI: 10.4149/neo_2015_050

33 Wang G, Chen H, Huang M, Wang N, Zhang J, Zhang Y, Bai G, Fong WF, Yang M and Yao X: Methyl protodioscin induces G2/M cell cycle arrest and apoptosis in HepG2 liver cancer cells. Cancer Lett *241(1)*: 102-109, 2006. PMID: 16458429. DOI: 10.1016/j.canlet.2005.10.050

34 Li X, Qu Z, Jing S, Li X, Zhao C, Man S, Wang Y and Gao W: Dioscin-6'-O-acetate inhibits lung cancer cell proliferation via inducing cell cycle arrest and caspase-dependent apoptosis. Phytomedicine *53*: 124-133, 2019. PMID: 30668391. DOI: 10.1016/j.phymed.2018.09.033

35 Wang P, Ding X, Kim H, Michalek SM and Zhang P: Structural effect on adjuvanticity of saponins. J Med Chem *63(6)*: 3290-3297, 2020. PMID: 32101001. DOI: 10.1021/acs.jmedchem.9b02063

36 Alexyuk PG, Bogoyavlenskiy AP, Alexyuk MS, Turmagambetova AS, Zaitseva IA, Omirtaeva ES and Berezin VE: Adjuvant activity of multimolecular complexes based on Glycyrrhiza glabra saponins, lipids, and influenza virus glycoproteins. Arch Virol *164(7)*: 1793-1803, 2019. PMID: 31079211. DOI: 10.1007/s00705-019-04273-2

37 Wei WC, Wang JH, Aravindaram K, Wang SJ, Hsu CC, Li CJ, Wen CC, Sheu JH and Yang NS: Polysaccharides from dioscorea

(shān yào) and other phytochemicals enhance antitumor effects induced by DNA vaccine against melanoma. J Tradit Complement Med *4(1)*: 42-48, 2014. PMID: 24872932. DOI: 10.4103/2225-4110.124342

38 Wang P: Natural and synthetic saponins as vaccine adjuvants. Vaccines (Basel) *9(3)*: 222, 2021. PMID: 33807582. DOI: 10.3390/vaccines9030222

39 Tian JH, Patel N, Haupt R, Zhou H, Weston S, Hammond H, Logue J, Portnoff AD, Norton J, Guebre-Xabier M, Zhou B, Jacobson K, Maciejewski S, Khatoon R, Wisniewska M, Moffitt W, Kluepfel-Stahl S, Ekechukwu B, Papin J, Boddapati S, Jason Wong C, Piedra PA, Frieman MB, Massare MJ, Fries L, Bengtsson KL, Stertman L, Ellingsworth L, Glenn G and Smith G: SARS-CoV-2 spike glycoprotein vaccine candidate NVX-CoV2373 immunogenicity in baboons and protection in mice. Nat Commun *12(1)*: 372, 2021. PMID: 33446655. DOI: 10.1038/s41467-020-20653-8

40 Richou R, Jensen R and Belin C: [Research on saponin, an adjuvant substance which stimulates immunity. I]. Rev Immunol Ther Antimicrob *28*: 49-62, 1964. PMID: 14187805.

41 Kensil CR: Saponins as vaccine adjuvants. Crit Rev Ther Drug Carrier Syst *13(1-2)*: 1-55, 1996. PMID: 8853958.

42 Wang P, Škalamera Đ, Sui X, Zhang P and Michalek SM: Synthesis and evaluation of QS-7-based vaccine adjuvants. ACS Infect Dis *5(6)*: 974-981, 2019. PMID: 30920199. DOI: 10.1021/acsinfecdis.9b00039

43 Aguado-Martínez A, Basto AP, Müller J, Balmer V, Manser V, Leitão A and Hemphill A: N-terminal fusion of a toll-like receptor 2-ligand to a Neospora caninum chimeric antigen efficiently modifies the properties of the specific immune response. Parasitology *143(5)*: 606-616, 2016. PMID: 26932317. DOI: 10.1017/S0031182016000056

44 Morein B, Hu KF and Abusugra I: Current status and potential application of ISCOMs in veterinary medicine. Adv Drug Deliv Rev *56(10)*: 1367-1382, 2004. PMID: 15191787. DOI: 10.1016/j.addr.2004.02.004

45 Hao Hao LX and Zhao XH: Report - In vitro immune potentials of a water-soluble polysaccharide extract from *Dioscorea* opposita planted in Henan Province, China. Pak J Pharm Sci *30(4)*: 1383-1388, 2017. PMID: 29039342.

46 Lee BH, Hsu WH, Liao TH and Pan TM: Inhibition of leukemia proliferation by a novel polysaccharide identified from Monascus-fermented dioscorea via inducing differentiation. Food Funct *3(7)*: 758-764, 2012. PMID: 22584829. DOI: 10.1039/c2fo30026e

47 Panthong S, Ruangnoo S, Thongdeeying P, Sriwanthana B and Itharat A: Immunomodulatory activity of *Dioscorea* membranacea Pierre rhizomes and of its main active constituent *Dioscorea*lide B. BMC Complement Altern Med *14*: 403, 2014. PMID: 25318548. DOI: 10.1186/1472-6882-14-403

48 Huong PT and Jeon YJ: Macrophage activation by glycoprotein isolated from *Dioscorea* batatas. Toxicol Res *27(3)*: 167-172, 2011. PMID: 24278568. DOI: 10.5487/TR.2011.27.3.167

49 Huong PT, Lee CH, Li MH, Lee MY, Kim JK, Lee SM, Seon JH, Lee DC and Jeon YJ: Characterization and immunopotentiating effects of the glycoprotein isolated from dioscorea batatas. Korean J Physiol Pharmacol *15(2)*: 101-106, 2011. PMID: 21660150. DOI: 10.4196/kjpp.2011.15.2.101

50 Giordano G, Segal L, Prinsen M, Wijnands MV, Garçon N and Destexhe E: Non-clinical safety assessment of single and repeated administration of gE/AS01 zoster vaccine in rabbits. J Appl Toxicol *37(2)*: 132-141, 2017. PMID: 27172098. DOI: 10.1002/jat.3329

51 Shi S, Zhu H, Xia X, Liang Z, Ma X and Sun B: Vaccine adjuvants: Understanding the structure and mechanism of adjuvanticity. Vaccine *37(24)*: 3167-3178, 2019. PMID: 31047671. DOI: 10.1016/j.vaccine.2019.04.055

52 Fochesato M, Dendouga N and Boxus M: Comparative preclinical evaluation of AS01 versus other Adjuvant Systems in a candidate herpes zoster glycoprotein E subunit vaccine. Hum Vaccin Immunother *12(8)*: 2092-2095, 2016. PMID: 26933767. DOI: 10.1080/21645515.2016.1154247

53 Sharma R, Palanisamy A, Dhama K, Mal G, Singh B and Singh KP: Exploring the possible use of saponin adjuvants in COVID-19 vaccine. Hum Vaccin Immunother *16(12)*: 2944-2953, 2020. PMID: 33295829. DOI: 10.1080/21645515.2020.1833579

54 He LX, Zhang ZF, Sun B, Chen QH, Liu R, Ren JW, Wang JB and Li Y: Sea cucumber (Codonopsis pilosula) oligopeptides: immunomodulatory effects based on stimulating Th cells, cytokine secretion and antibody production. Food Funct *7(2)*: 1208-1216, 2016. PMID: 26838796. DOI: 10.1039/c5fo01480h

55 Peng Y, Song Y, Wang Q, Hu Y, He Y, Ren D, Wu L, Liu S, Cong H and Zhou H: *In vitro* and *in vivo* immunomodulatory effects of fucoidan compound agents. Int J Biol Macromol *127*: 48-56, 2019. PMID: 30593813. DOI: 10.1016/j.ijbiomac.2018.12.197

56 Wang J, Tong X, Li P, Liu M, Peng W, Cao H and Su W: Bioactive components on immuno-enhancement effects in the traditional Chinese medicine Shenqi Fuzheng Injection based on relevance analysis between chemical HPLC fingerprints and in vivo biological effects. J Ethnopharmacol *155(1)*: 405-415, 2014. PMID: 24950446. DOI: 10.1016/j.jep.2014.05.038

57 Bamodu OA, Kuo KT, Wang CH, Huang WC, Wu ATH, Tsai JT, Lee KY, Yeh CT and Wang LS: *Astragalus polysaccharides* (PG2) enhances the M1 polarization of macrophages, functional maturation of dendritic cells, and T cell-mediated anticancer immune responses in patients with lung cancer. Nutrients *11(10)*: 2264, 2019. PMID: 31547048. DOI: 10.3390/nu11102264

58 Tian Y, Li X, Li H, Lu Q, Sun G and Chen H: Astragalus mongholicus regulate the Toll-like-receptor 4 meditated signal transduction of dendritic cells to restrain stomach cancer cells. Afr J Tradit Complement Altern Med *11(3)*: 92-96, 2014. PMID: 25371568. DOI: 10.4314/ajtcam.v11i3.13

59 Salemme V, Centonze G, Cavallo F, Defilippi P and Conti L: The crosstalk between tumor cells and the immune microenvironment in breast cancer: Implications for immunotherapy. Front Oncol *11*: 610303, 2021. PMID: 33777750. DOI: 10.3389/fonc.2021.610303

60 Steven A and Seliger B: The role of immune escape and immune cell infiltration in breast cancer. Breast Care (Basel) *13(1)*: 16-21, 2018. PMID: 29950962. DOI: 10.1159/000486585

61 Gross S and Walden P: Immunosuppressive mechanisms in human tumors: why we still cannot cure cancer. Immunol Lett *116(1)*: 7-14, 2008. PMID: 18164076. DOI: 10.1016/j.imlet.2007.11.012

62 Li X, Yao W, Yuan Y, Chen P, Li B, Li J, Chu R, Song H, Xie D, Jiang X and Wang H: Targeting of tumour-infiltrating macrophages via CCL2/CCR2 signalling as a therapeutic strategy against hepatocellular carcinoma. Gut *66(1)*: 157-167, 2017. PMID: 26452628. DOI: 10.1136/gutjnl-2015-310514

63 Heiskala M, Leidenius M, Joensuu K and Heikkilä P: High expression of CCL2 in tumor cells and abundant infiltration with CD14 positive macrophages predict early relapse in breast cancer. Virchows Arch *474(1)*: 3-12, 2019. PMID: 30368555. DOI: 10.1007/s00428-018-2461-7

64 Ohashi T, Inoue N and Aoki M: The Warburg Effect and M2 Macrophage Polarization in Head and Neck Cancer. Gan To Kagaku Ryoho *47(1)*: 6-10, 2020. PMID: 32381853.

65 Vendramini-Costa DB and Carvalho JE: Molecular link mechanisms between inflammation and cancer. Curr Pharm Des *18(26)*: 3831-3852, 2012. PMID: 22632748. DOI: 10.2174/138161212802083707

66 Mohamed MM, El-Ghonaimy EA, Nouh MA, Schneider RJ, Sloane BF and El-Shinawi M: Cytokines secreted by macrophages isolated from tumor microenvironment of inflammatory breast cancer patients possess chemotactic properties. Int J Biochem Cell Biol *46*: 138-147, 2014. PMID: 24291763. DOI: 10.1016/j.biocel.2013.11.015

67 Sousa S, Brion R, Lintunen M, Kronqvist P, Sandholm J, Mönkkönen J, Kellokumpu-Lehtinen PL, Lauttia S, Tynninen O, Joensuu H, Heymann D and Määttä JA: Human breast cancer cells educate macrophages toward the M2 activation status. Breast Cancer Res *17*: 101, 2015. PMID: 26243145. DOI: 10.1186/s13058-015-0621-0

68 Myers KV, Pienta KJ and Amend SR: Cancer cells and M2 macrophages: Cooperative invasive ecosystem engineers. Cancer Control *27(1)*: 1073274820911058, 2020. PMID: 32129079. DOI: 10.1177/1073274820911058

69 Yang M, Liu J, Shao J, Qin Y, Ji Q, Zhang X and Du J: Cathepsin S-mediated autophagic flux in tumor-associated macrophages accelerate tumor development by promoting M2 polarization. Mol Cancer *13*: 43, 2014. PMID: 24580730. DOI: 10.1186/1476-4598-13-43

70 Xu J, Yu Y, He X, Niu N, Li X, Zhang R, Hu J, Ma J, Yu X, Sun Y, Ni H and Wang F: Tumor-associated macrophages induce invasion and poor prognosis in human gastric cancer in a cyclooxygenase-2/MMP9-dependent manner. Am J Transl Res *11(9)*: 6040-6054, 2019. PMID: 31632572.

71 Vinnakota K, Zhang Y, Selvanesan BC, Topi G, Salim T, Sand-Dejmek J, Jönsson G and Sjölander A: M2-like macrophages induce colon cancer cell invasion via matrix metalloproteinases. J Cell Physiol *232(12)*: 3468-3480, 2017. PMID: 28098359. DOI: 10.1002/jcp.25808

72 You D, Jeong Y, Yoon SY, Kim SA, Lo E, Kim SW, Lee JE, Nam SJ and Kim S: Entelon® (*Vitis vinifera* seed extract) prevents cancer metastasis via the downregulation of Interleukin-1 alpha in triple-negative breast cancer cells. Molecules *26(12)*: 3644, 2021. PMID: 34203721. DOI: 10.3390/molecules26123644

73 Seliger B and Massa C: Immune therapy resistance and immune escape of tumors. Cancers (Basel) *13(3)*: 551, 2021. PMID: 33535559. DOI: 10.3390/cancers13030551

74 Sanchez CE, Dowlati EP, Geiger AE, Chaudhry K, Tovar MA, Bollard CM and Cruz CRY: NK cell adoptive immunotherapy of cancer: Evaluating recognition strategies and overcoming limitations. Transplant Cell Ther *27(1)*: 21-35, 2021. PMID: 33007496. DOI: 10.1016/j.bbmt.2020.09.030

75 Tonn T, Becker S, Esser R, Schwabe D and Seifried E: Cellular immunotherapy of malignancies using the clonal natural killer cell line NK-92. J Hematother Stem Cell Res *10(4)*: 535-544, 2001. PMID: 11522236. DOI: 10.1089/15258160152509145

76 Biswas BK, Guru SA, Sumi MP, Jamatia E, Gupta RK, Lali P, Konar BC, Saxena A and Mir R: Natural killer cells expanded and preactivated exhibit enhanced antitumor activity against different tumor cells *in vitro*. Asian Pac J Cancer Prev *21(6)*: 1595-1605, 2020. PMID: 32592353. DOI: 10.31557/APJCP.2020.21.6.1595

77 Abbott RC, Cross RS and Jenkins MR: Finding the keys to the CAR: Identifying novel target antigens for T cell redirection immunotherapies. Int J Mol Sci *21(2)*: 515, 2020. PMID: 31947597. DOI: 10.3390/ijms21020515

78 Sommaggio R, Cappuzzello E, Dalla Pietà A, Tosi A, Palmerini P, Carpanese D, Nicolè L and Rosato A: Adoptive cell therapy of triple negative breast cancer with redirected cytokine-induced killer cells. Oncoimmunology *9(1)*: 1777046, 2020. PMID: 32923140. DOI: 10.1080/2162402X.2020.1777046

79 Lee H, Kim YA, Kim Y, Park HS, Seo JH, Lee H, Gong G and Lee HJ: Clinicopathological factors associated with tumor-infiltrating lymphocyte reactivity in breast cancer. Cancer Immunol Immunother *69(11)*: 2381-2391, 2020. PMID: 32529292. DOI: 10.1007/s00262-020-02633-5

80 Wang ZX, Cao JX, Wang M, Li D, Cui YX, Zhang XY, Liu JL and Li JL: Adoptive cellular immunotherapy for the treatment of patients with breast cancer: a meta-analysis. Cytotherapy *16(7)*: 934-945, 2014. PMID: 24794183. DOI: 10.1016/j.jcyt.2014.02.011

81 Yang L, Lou M, Liu W, Feng D, Cheng T and Ma J: Amplification of immune cells derived from human peripheral blood and cytotoxicity on MDA-MB-231 breast cancer cells *in vitro*. Xi Bao Yu Fen Zi Mian Yi Xue Za Zhi *35(8)*: 682-688, 2019. PMID: 31638564.

82 Shi YJ, Ren HY, Cen XN, Dong YJ, Ma MX, Zhao YL, Zhu Y and Yu JR: [Dendritic cells elicit cellular immune response by targeting to capture breast cancer cells]. Zhonghua Zhong Liu Za Zhi *30(2)*: 107-111, 2008. PMID: 18646691.

83 Pan K, Guan XX, Li YQ, Zhao JJ, Li JJ, Qiu HJ, Weng DS, Wang QJ, Liu Q, Huang LX, He J, Chen SP, Ke ML, Zeng YX and Xia JC: Clinical activity of adjuvant cytokine-induced killer cell immunotherapy in patients with post-mastectomy triple-negative breast cancer. Clin Cancer Res *20(11)*: 3003-3011, 2014. PMID: 24668644. DOI: 10.1158/1078-0432.CCR-14-0082

Received July 23, 2021
Revised August 29, 2021
Accepted September 23, 2021